Nebraska Transportation Center

MID-AMERICA TRANSPORTATION CENTER

NDOR Nebraska Department of Roads

Report SPR-P1(16) M043

Final Report
26-1121-4030-001

Condition Factor Calibration for Load and Resistance Factor Rating of Steel Girder Bridges

Joshua Steelman, Ph.D.
Assistant Professor
Department of Civil Engineering
University of Nebraska-Lincoln

Pranav Shakya
Graduate Research Assistant
Department of Civil Engineering
University of Nebraska-Lincoln

2017

Nebraska Transportation Center
262 Prem S. Paul Research Center at Whittier School
2200 Vine Street
Lincoln, NE 68583-0851
(402) 472-0141

"This report was funded in part through grant[s] from the Federal Highway Administration [and Federal Transit Administration], U.S. Department of Transportation. The views and opinions of the authors [or agency] expressed herein do not necessarily state or reflect those of the U.S. Department of Transportation."

Condition Factor Calibration for

Load and Resistance Factor Rating of Steel Girder Bridges

Joshua Steelman, Ph.D.
Assistant Professor
Department of Civil Engineering
University of Nebraska-Lincoln

Pranav Shakya
Graduate Research Assistant
Department of Civil Engineering
University of Nebraska-Lincoln

A Report on Research Sponsored by

Mid-American Transportation Center

University of Nebraska-Lincoln

June 2017

Technical Report Documentation Page

1. Report No SPR-P1 (16) M043	2. Government Accession No.	3. Recipient's Catalog No.	
4. Title and Subtitle Condition Factor Calibration for Load and Resistance Factor Rating of Steel Girder Bridges		5. Report Date June 2016	
		6. Performing Organization Code 26-1121-4030-001	
7. Authors Joshua Steelman, Pranav Shakya		8. Performing Organization Report No.	
9. Performing Organization Name and Address University of Nebraska-Lincoln Nebraska Transportation Center 2200 Vine St. 262 Whittier Research Center PO Box 830851 Lincoln, NE 68583-0851		10. Work Unit No. (TRAIS)	
		11. Contract or Grant No.	
12. Sponsoring Organization Name and Address Nebraska Department of Roads 1500 Hwy. 2 Lincoln, NE 68502		13. Type of Report and Period Covered July 2015-December 2016	
		14. Sponsoring Agency Code MATC TRB RiP No. 36240	
15. Supplementary Notes			
16. Abstract Load and Resistance Factor Rating (LRFR) is a reliability-based rating procedure complementary to Load and Resistance Factor Design (LRFD). The intent of LRFR is to provide consistent reliability for all bridges regardless of in-situ condition. The primary difference between design and rating is the uncertain severity and location of deterioration, including the potential future loss of strength for an element already evidencing deterioration. Ostensibly, these uncertainties are addressed by applying an additional strength reduction factor: the condition factor, ϕ_c. Currently, condition factors are nominally correlated to the condition of the member, which can be Good, Fair, or Poor. However, definitions of these condition categories are deferred to inspection documents, which themselves lack clear, objective definitions. Furthermore, lack of guidance to account for the location and extent of deterioration exacerbates confusion in the methodology to appropriately assign condition factors. These ambiguities cause incoherence between inspection and rating processes by introducing additional uncertainty. The additional uncertainty skews load ratings, sometimes producing ratings with unintended conservativism, and sometimes overestimating the safe load-carrying capacity of a bridge. This study presents a calibration of ϕ_c to be used with steel girder bridges, accounting for uncertainty due to non-uniform deterioration throughout transverse sections, unquantified severity of section loss associated with condition states, lack of knowledge of the longitudinal location(s) of the deterioration, and the likelihood of further deterioration over the next inspection cycle for ranges of section loss for each condition. The proposed condition state definitions and implementation methodology are intended to improve uniformity in the inspection process and produce bridge load ratings that are more consistent with the target reliability intended by the LRFR rating procedure.			
17. Key Words Steel girder, LRFR, rating, reliability, condition factor	18. Distribution Statement		
19. Security Classification (of this report) Unclassified	20. Security Classification (of this page) Unclassified	21. No. Of Pages 108	22. Price

Form DOT F 1700.7 (8-72) Reproduction of form and completed page is authorized

Table of Contents

List of Figures

List of Tables

Disclaimer

The contents of this report reflect the views of the authors, who are responsible for the facts and accuracy of the information presented herein. This document is disseminated under the sponsorship of the U.S. Department of Transportation's University Transportation Centers Program, in the interest of information exchange. The U.S. Government assumes no liability for the contents of use thereof.

Abstract

Load and Resistance Factor Rating (LRFR) is a reliability-based rating procedure complementary to Load and Resistance Factor Design (LRFD). The intent of LRFR is to provide consistent reliability for all bridges regardless of in-situ condition. The primary difference between design and rating is the uncertain severity and location of deterioration, including the potential future loss of strength for an element already evidencing deterioration. Ostensibly, these uncertainties are addressed by applying an additional strength reduction factor: the condition factor, ϕ_c. Currently, condition factors are nominally correlated to the condition of the member, which can be Good, Fair, or Poor. However, definitions of these condition categories are deferred to inspection documents, which themselves lack clear, objective definitions. Furthermore, lack of guidance to account for the location and extent of deterioration exacerbates confusion in the methodology to appropriately assign condition factors. These ambiguities cause incoherence between inspection and rating processes by introducing additional uncertainty. The additional uncertainty skews load ratings, sometimes producing ratings with unintended conservativism, and sometimes overestimating the safe load-carrying capacity of a bridge. This study presents a calibration of ϕ_c to be used with steel girder bridges, accounting for uncertainty due to non-uniform deterioration throughout transverse sections, unquantified severity of section loss associated with condition states, lack of knowledge of the longitudinal location(s) of the deterioration, and the likelihood of further deterioration over the next inspection cycle for ranges of section loss for each condition. The proposed condition state definitions and implementation methodology are intended to improve uniformity in the inspection process and produce bridge load ratings that are more consistent with the target reliability intended by the LRFR rating procedure.

Chapter 1: Introduction

Bridge inspections and evaluations are performed to establish the safe load-carrying capacity of bridges, accounting for, among other things, new and ongoing deterioration. AASHTO LRFD imposes an implicit acceptable level of reliability for bridges and their components at the design stage to ensure sufficient safety. Reliability is defined by achieving an acceptably small probability of failure, which requires the quantification of demand and capacity means (expected values) and dispersions (uncertainties). Corrosion both decreases the expected value and increases the uncertainty in capacity.

The American Association of State Highway and Transportation Officials (AASHTO) Manual for Bridge Evaluation (MBE) requires load rating to be performed using the Allowable Stress Rating (ASR), Load Factor Rating (LFR) or Load and Resistance Rating Factor (LRFR) (AASHTO, 2014). LRFR is the most recently developed among these methods, and parallels LRFD (the preferred method for design of AASHTO). NDOR has adopted LRFD for the design of new bridges since 2010, so it is expected that LRFR will be used increasingly in the future to evaluate aging bridges designed according to LRFD.

LRFR fundamentally seeks to maintain consistent reliability across all bridges, including accounting for deteriorated structural elements. Section 6A.4.2.3 of the MBE introduces the condition factor, ϕ_c, to account for "increased uncertainty in the resistance of deteriorated members and the likely increased future deterioration of these members during the period between inspection cycles." (AASHTO, 2014).

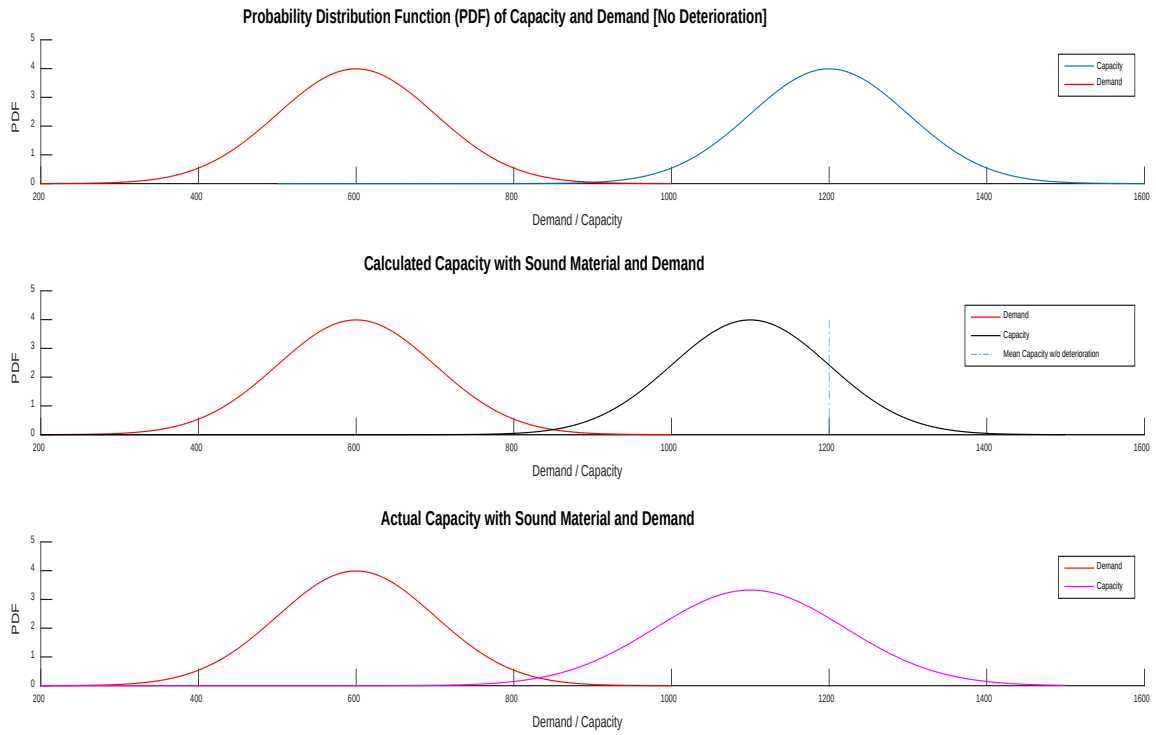

Figure 1.1 The purpose of ϕ_c

Figure 1.1 illustrates the concepts and intent underlying ϕ_c. The first graph in the figure shows the variable demand and capacity of a new girder. Failure occurs when demand (an uncertain value, represented by the red/left probability distribution) exceeds capacity (also an uncertain value, represented by the blue/right probability distribution). As the girder deteriorates, capacity decreases, resulting in a shift of the capacity curve to the left, as seen in the second graph. In the second graph, capacity is calculated using the remaining section (i.e., sound material area), but this assessment does not capture the increased uncertainty in capacity due to deterioration. The third graph has a higher dispersion in the capacity (quantified by a higher standard deviation), which captures the increased uncertainty associated with deterioration. ϕ_c shifts the deterministic "capacity" used in rating downward to reflect this increased uncertainty and the consequently higher probability of failure.

Increased uncertainty in deteriorated girder capacity results from:

- non-uniform deterioration across any given girder cross-section
- uncertain location of deteriorated conditions along the span
- likelihood of future deterioration
- human error during inspections

NCHRP 301 by Moses and Verma first introduced the condition factor. The primary intent and basis for the condition factor was to account for future corrosion in a girder, depending on various environmental factors. NCHRP 301 identified three general categories to represent a range of corrosive environments: rural, industrial, and marine. These corrosive environment classifications approximately correspond to the three condition states currently recognized by the MBE as the determinants for ϕ_c: "Good or Satisfactory", "Fair", and "Poor". The recommended values in NCHRP 301 reflected observations of varying losses from a field test program that subjected steel plate specimens to various corrosive environment scenarios.

Inspection detail varies with the type of inspection performed in the field (e.g., routine versus special) and with the individual performing the inspection, producing additional uncertainty in capacity from bridge to bridge. Pertinent inspection details for the characterization of ϕ_c include the spatial dispersion and severity of deterioration. The inspector typically notes some information regarding section loss during the inspection, but either or both the location and severity of the deterioration may be omitted from the inspection report.

In a new bridge, the critical location for all the modes of failures (flexure, shear, bearing) are known. For example, the location of the minimum load to capacity ratio is near the mid-span because the uniform cross-section of a new girder provides uniform load capacity along the span. The same girder after deterioration would have non-uniform load carrying capacity, which could

move the critical location away from the mid-span. If the cross-section along the span is unknown, there will be uncertainty in the location of the critical section.

The MBE defers the task of providing member condition definitions (Good versus Fair versus Poor) to the Manual for Bridge Element Inspection (MBEI). However, the MBEI also lacks clarity and objective definitions. Furthermore, lack of guidance to account for the location and the extent of deterioration exacerbates confusion when classifying the member into one of the three general conditions. In practical terms, the problem is that load ratings produced based on existing guidance in MBE and MBEI do not consistently provide the target level of reliability, as intended by the LRFR procedure.

The problem is complex, and it is not possible to conclusively say that the current guidance for load ratings produces either conservative or unconservative estimates of load ratings, because the outcome will vary from bridge to bridge. However, it would be reasonable to presume that the current format and practices would in general produce significantly conservative load ratings. Deteriorated conditions at a support should rationally be reflected in shear and bearing limit states only, if deterioration near midspan is negligible. Instead, a superstructure assessed to have a condition lower than “Good” will need to be evaluated with a ϕ_c penalty to all limit states. A bridge could require load restriction on this basis of unfairly penalized flexural strength, even though the deterioration at supports is insufficient to compromise shear and/or bearing severely enough to control over (actual, non-deteriorated) flexure, and deterioration is in fact negligible in the load carrying capacity of the structure. This outcome must necessarily disincentivize use of LRFR as a result of insufficient guidance for the application of ϕ_c.

The objective of this research is to provide a procedure to select a calibrated ϕ_c appropriate to field conditions, accounting for the uncertainty due to non-uniform deterioration in the girder across a section, the lack of knowledge of the location of the deterioration, and the likelihood of further deterioration over the next inspection cycle. To address these challenges, the following four objectives were identified:

1. survey, describe, and categorize inspection methods, policies, and procedures used by NDOR;
2. identify and categorize types of corrosion commonly observed for steel girder bridges;
3. formulate and assess the relationship between deterioration, loss of capacity, and increase in uncertainty; and
4. develop a procedure to map knowledge available from inspections to corresponding condition factors, ϕ_c, and the reduction in nominal capacity.

The scope of this study is constrained to:

- simple span girder bridges,
- rolled steel girders of mild steel with yield strengths of 36 ksi,
- carbon and weathering steel,
- projected future deterioration within a 2-year inspection cycle,
- composite girders with concrete slabs having depths of 8 inches and specified compressive strengths of 4 ksi,
- compact cross-sections in flexure, and
- consideration of flexural limit states.

Chapter 2: Literature Review

Calibration of ϕ_c requires an understanding of the bridge inspection and evaluation process, the effects of corrosion, and the use of ϕ_c in LRFR. Section 2.1 Overview of Bridge Inspection and Evaluation discusses the details of bridge inspection and evaluation. Section 2.2 Deterioration Mechanisms and Rates provides a description of the effects of corrosion in the steel bridges, the rate of corrosion for carbon and weathering steels, and documented patterns of corrosion seen in the field. Section 2.3 Development of LRFR provides a summary of the LRFR load rating procedure, along with the history of the ϕ_c. Finally, section 2.4 Steel Bridge Reliability discusses previous studies on the effects of corrosion on steel bridge reliability.

2.1 Overview of Bridge Inspection and Evaluation

The Federal Highway Act of 1968 required the Secretary of Transportation to establish a National Bridge Inspection Standard (NBIS) in 1971. The NBIS established a national policy regarding inspection procedures, the frequency of inspections, qualifications of personnel, inspection reports, and maintenance of state bridge inventory (Federal Highway Administration, 2012). Over time, the Federal Highway Administration (FHWA) has developed reference manuals, including the Bridge Inspector's Training Manual 70, Manual for Maintenance of Bridges, Recording and Coding Guide for the Structure Inventory and Appraisal of the Nation's Bridges, The Bridge Inspector's Manual for Movable Bridges, Culvert Inspection Manual, Inspection of Fracture Critical Bridge Members, etc. A selection of the current FHWA reference materials are discussed below: (Federal Highway Administration, 2012)

- Bridge Inspector's Reference Manual (BRIM)

A manual for inspectors that includes: a bridge inspection program; safety fundamentals for bridge inspectors; bridge terminology; bridge inspection reporting; bridge mechanics; bridge materials, inspection and evaluation guidance for bridge decks and areas adjacent to bridge

decks; inspection and evaluation guidance for superstructures, bridge bearings, and substructures; characteristics, inspection and evaluation of culverts; and advanced inspection methods for complex bridges.

- Manual for Bridge Element Inspection (MBEI):

The MBEI defines a comprehensive set of elements, and is intended to be flexible in nature to satisfy the needs of all agencies. Elements are characterized into four general condition assessment categories: Good, Fair, Poor and Severe. Criteria and definitions for each condition state are defined separately for each type of element.

- Manual for Bridge Evaluation (MBE):

The MBE is a standard for providing uniformity in the procedures and policies used to determine the physical condition, maintenance needs, and load capacity of the nation's highway bridges. It assists bridge owners by establishing inspection procedures and evaluation practices that meet the NBIS.

- Recording and Coding Guide for the Structure Inventory and Appraisal (SI&A) of the Nation's Bridges:

This guide has been prepared for state, federal, and other agencies to use for recording and coding the data elements that will comprise the NBI database. This guide is used to formulate an accurate report for Congress on the quantity and condition of the nation's bridges. The coded items in this guide are considered an integral part of the database that can be used to meet several federal reporting requirements, as well as part of the states' needs. This guide is used to generate reports to be submitted to the Highway Bridge Replacement and Rehabilitation Program and the National Bridge Inspection Program (Weseman, 1995). The broad NBI condition ratings (superstructure, substructure, and deck) have been collected for all bridges, both on and off the National Highway System (NHS) since the NBIS was established in 1971.

Condition ratings and other functional and geometric bridge data is used by FHWA to determine Sufficiency Ratings for funding prioritization (Bridge Inspection Manual NDOR).

- Code of Federal Regulation:

The purpose of the regulations in this part is to implement and carry out the provisions of federal law relating to the administration of federal aid for highways. This federal aid policy guide describes the process followed by FHWA when distributing federal funding to the states for transportation. It also contains requirements that the state governments need to fulfill for the federal funding (Federal Highway Administration, 2010).

2.1.1 Bridge Inspection Types and Reporting

The MBE requires that bridges be inspected at regular intervals, not to exceed 24 months without prior approval from FHWA and justification by past reports and performance history and analysis. MBE describes various types of inspections, including initial inspections, routine inspections, damage inspections, in-depth inspections, fracture-critical inspections, underwater inspections, and special inspections.

The types of inspections require various levels of rigor with respect to details about a bridge and its elements. There are two major types of routine inspections: Structure Inventory and Appraisal (SI&A) and Element Level Inspection. These inspections have fundamentally different inspection reporting techniques. SI&A reports the overall condition of bridge parts like the superstructure, the substructure, or the deck. Element Level Inspection requires reports of the condition of all bridge elements, such as girders, abutments, piers, etc.

NDOR inspections include the SI&A bridge condition ratings for reporting to NBI, but load ratings are typically evaluated using Element Inspection data.

Use of Element Level Inspection allows NDOR to manage their bridge inventory more effectively by:

- quantifing and describing element conditions observed during the inspection and the extent of deterioration;
- identifing candidates for preservation, maintenance, rehabilitation, improvement (i.e. widening, raising, strengthening) and replacement practices/strategies;
- predicting future deterioration of bridge elements for scheduling purposes; and
- managing their budgets for bridge preservation.

(Nebraska Department of Roads: Bridge Division, 2015)

2.2 Deterioration Mechanisms and Rates

The MBEI requires inspection of all elements for various defects including corrosion, cracking, connection defects, delamination/spall/patched area, efflorescence/rust staining, cracking, deterioration, distortion, and damage. The most common form of deterioration identified in inspections of steel girders is corrosion – the oxidization of metal through a reaction involving oxygen, water, or other agents. Corrosion is an electrochemical process between two metals: the metal components having a higher tendency to corrode (anode) and the metal components having a lower tendency to corrode (cathode). When an electrolyte is present, current flows and oxidation occurs. The electrolyte usually present on bridges is water (Kulicki, Prucz, Sorgenfrei, Mertz, & Young, 1990). While corrosion can occur through a variety of mechanisms (galvanic corrosion, crevice corrosion, pitting, intergranular corrosion, selective leaching, erosion corrosion, stress corrosion, hydrogen damage), all corrosion mechanisms cause section loss, and it is not necessary to consider each individually.

NCHRP report 333 addressed four major corrosion effects: loss of section, creation of stress concentration, introduction of unintended fixity, and introduction of unintended movement (Kulicki et al., 1990). The loss of section reduces the geometric properties, such as the moment of inertia, radius of gyration, slenderness ratio of the web, and flanges (Kayser & Nowak, 1989a). This reduction lowers the bending, axial and shear capacity of the member, and can also affect the fatigue life of the member because of the increased stress range (Czarnecki & Nowak, 2008). Out of the four effects of corrosion, this study focused on the loss of section due to corrosion.

2.2.1 Rate of Corrosion

The rate of corrosion depends on an extensive list of parameters. One of the primary considerations is the presence of electrolytes, such as water, oxygen, and salt. Electrolyte concentration varies depending on the environment. Marine environments, for example, possess a higher abundance of water and salt, and therefore experience a significantly increased rate of corrosion (Kayser & Nowak, 1989a). Komp (1987) studied corrosion rates for various metals and environments, including carbon and weathering steels, and rural, urban, and marine environments. Komp proposed an asymptotic function, shown in Eqn. (1), to predict the corrosion in metal. Parameters A and B are specific to the type of steel and environment, as shown in Table 2.1. The equation captures the decreasing corrosion rate over time from field observations with B coefficients less than unity.

$$C = At^B \tag{1}$$

$Where\ C\ is\ the\ average\ corrosion\ penetration\ in\ microns$

$t\ is\ the\ number\ of\ years$

$A\ and\ B\ correspond\ to\ steel\ type\ and\ environment$

Table 2-1 Corrosion parameters in Komp's corrosion model

Environment	Carbon Steel		Weathering Steel	
	A	**B**	**A**	**B**
Rural	34.0	0.65	33.3	0.50
Urban	80.2	0.59	50.7	0.57
Marine	70.6	0.79	40.2	0.56

Komp's model is plotted for each combination of steel material and environment in Figure 2.1 and Figure 2.2. Although various models are available for corrosion rate prediction, researchers that have formerly studied bridge deterioration have frequently chosen to use Komp's model (Moses and Verma, 1987; McCrum, Arnold, and Dexter, 1985).

Komp followed ASTM G 50-10 "Standard Practice for Conducting Atmospheric Corrosion Tests on Metals" to evaluate the corrosion resistance of metals when exposed to weather, as well as to evaluate the relative corrosivity of the atmosphere at a specific location. The test sites – described as rural, industrial (urban), and marine atmospheres – were characterized in accordance with practice G92 "Practice for Characterization of Atmospheric Test Sites."

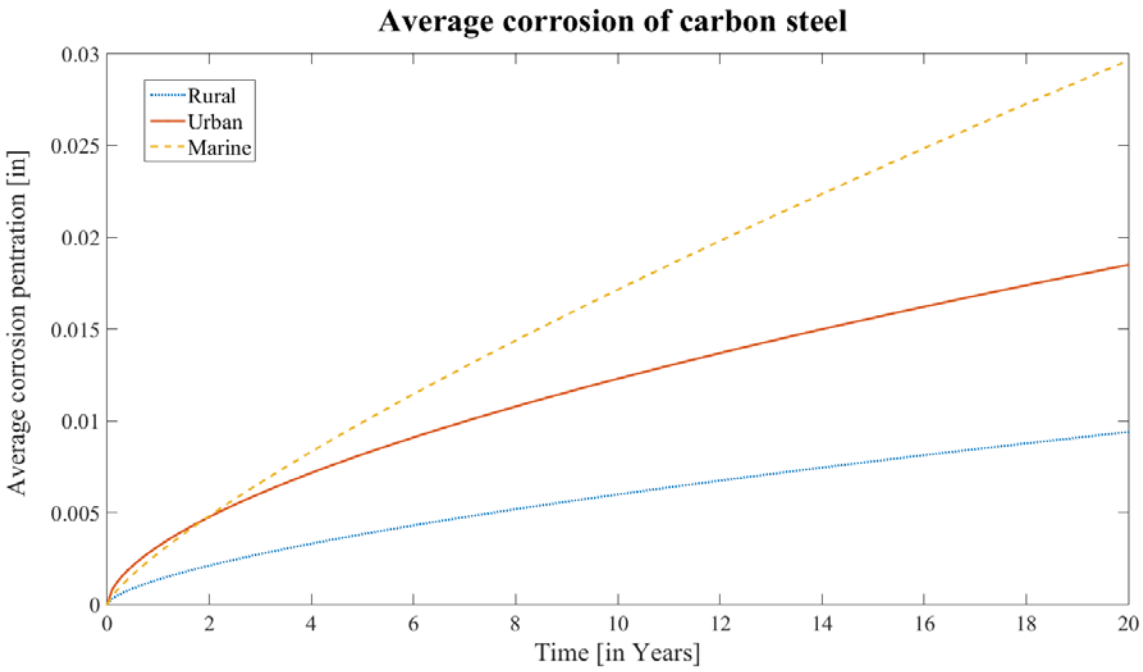

Figure 2.1 Average corrosion of carbon steel using Komp's model

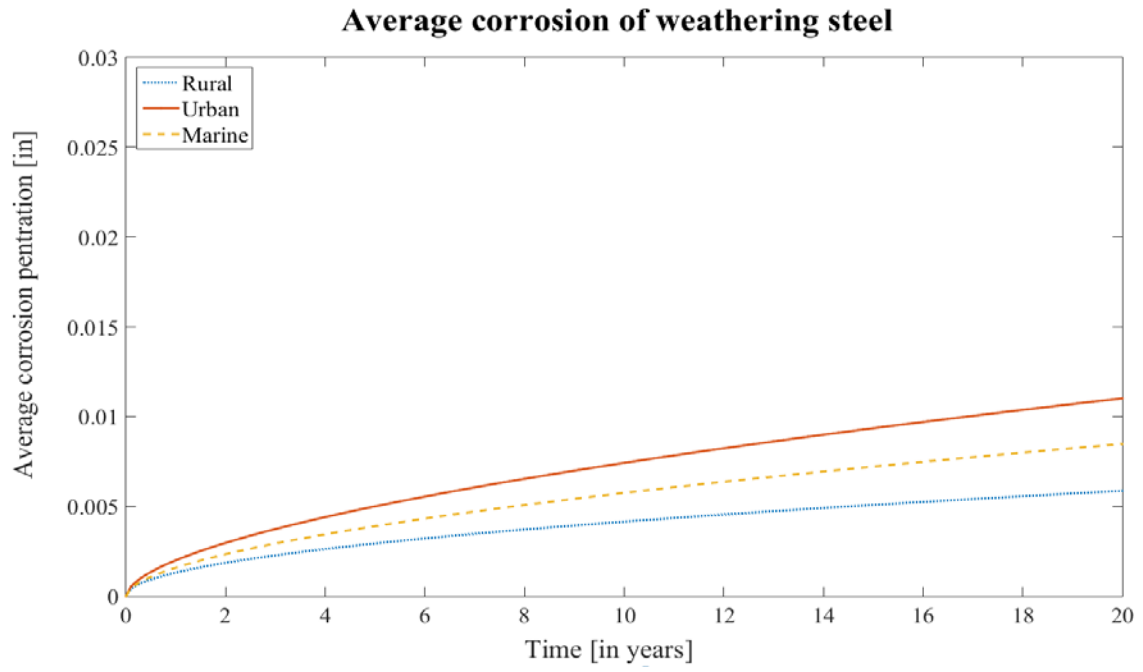

Figure 2.2 Average corrosion of weathering steel using Komp's model

Corrosion rate is typically expressed either as penetration per year or loss in thickness over a specified exposure period. ASTM G 50-10 defines corrosion rate as the average of the top and bottom surface losses for test samples (ASTM International, 2015). Corrosion rates are influenced by climate and shelter conditions, the orientation of exposed surfaces, the angle of exposure, and the presence of moisture and deicing salts. Out of these factors, shelter, orientation, and deicing salt more significantly affect the rate of corrosion. McKenzie suggested multipliers to modify corrosion rates for the sheltered versus exposed corrosion condition, as shown in Table 2.2. Lastly, deicing salts cause approximately 2.75 times more corrosion than the absence of salt, according to Albrecht and Naeemi (Albrecht & Naeemi, 1984; Moses & Verma, 1987).

Table 2-2 Corrosion penetration of sheltered VS exposed conditions

Environment	Corrosion for sheltered conditions Corrosion for exposed conditions
Rural	1.0
Industrial	1.7
Marine	2.0

2.3 Development of LRFR Methodology

The MBE describes three load rating procedures to establish bridge live load capacity. This research focuses on LRFR, which is intended to calculate the remaining live load capacity of a bridge with more consistent reliability than alternative methods (ASR and LFR). In the standard MBE load rating formulation, the dead and permanent loads are subtracted from the capacity and the remainder is then divided by the live load to calculate the load rating. A load rating value greater than 1 means that the bridge can reliably carry the design live load. A load

rating value less than 1 means that the bridge cannot reliably carry the traffic load modeled as live load and may need to be posted for a lower load to avoid failure.

The capacity term includes multiple factors: ϕ, ϕ_s, and ϕ_c. The ϕ factor is obtained from the corresponding LRFD limit state, and accounts for typical sources of capacity uncertainty recognized in design: fabrication tolerances (e.g., flange thickness), material properties (e.g., steel yield strength), and common professional assumptions (e.g., effective composite slab width). The system factor, ϕ_s, is typically a penalty for a lack of redundancy in the structure for the element under consideration. It is permitted to increase ϕ_s beyond 1, but the allowance is relegated to the commentary with little guidance to facilitate implementation. The condition factor, ϕ_c, accounts for the increased uncertainty associated with the deteriorated conditions. Additional details of load rating formulation and terms are presented in Chapter 4: Reliability Analysis.

LRFR addresses two levels of safety: inventory and operating. Safety is ensured at each of these levels by selecting particular values for a reliability index, which is a measure of the probability of failure. The inventory rating corresponds to a reliability index of 3.5 (0.023% probability of failure during the design life), and the operating rating corresponds to a reliability index of 2.5 (0.62% probability of failure). LRFD is calibrated to produce structures that satisfy inventory rating at design. AASHTO allows bridges to be rated at the lower operating target reliability level, justified with a biannual inspection. LRFR produces ratings corresponding to the respective rating levels by stipulating appropriately calibrated live load factors: 1.75 for live load in the Strength I combination at inventory level versus 1.35 at operating level. The resistance factor and other load factors do not change for the two rating levels.(AASHTO, 2014)

The LRFR condition factor accounts for the increased uncertainty in the capacity due to deterioration. Moses and Verma introduced the condition factor in NCHRP 301 to account for future corrosion. NCHRP 301 classified girder conditions into three categories: Good, Slight, and Severe. Corresponding "capacity reduction factors" are presented in Table 2.3. The capacity reduction factors are effectively ϕ_c values, but are referred to only as ϕ factors. NCHRP 301 pre-dated AASHTO LRFD, although the report notes that LRFD is used in other specifications, such as the material specifications produced by the American Institute of Steel Construction (AISC) and the American Concrete Institute (ACI).

Table 2-3 Condition rating and the penalization from NCHRP 301

Condition	Capacity Reduction Factor, ϕ
Good condition	0.95
Slight corrosion, some section loss	0.85
Severe corrosion, considerable section loss	0.75

NCHRP 301 used Komp's corrosion model (refer to 2.2.1 Rate of Corrosion) for various environments to estimate future corrosion, and assumed that environments corresponded to deteriorated girder conditions (see Table 2.4). The authors assumed that rural environments corrode to "Good" condition, urban environments corrode to "Slight" deterioration, and marine environments corrode to "Severe" condition. Estimated section losses in NCHRP 301 included multipliers to account for deicing salt and sheltered conditions (see 2.2.1 Rate of Corrosion). The amount of loss expected per side of a plate element over 2 years is summarized in Table 2.5 for each condition state. NCHRP 301 reported an estimated mean section modulus reduction for a W27x94, as reproduced in Table 2.6**.** (Moses & Verma, 1987).

Table 2-4 Corrosion rate for carbon steel for different corrosion of section

Corrosion of Section	Type of Environment	Eq. H-1
Normal, Good Condition	**Rural**	**C = 34 t0.65**
Medium, Slight Corrosion	**Industrial**	**C = 65 t0.5**
Severe Corrosion	**Marine**	**C = 80 t0.8**

Table 2-5 Calculation of average thickness loss for difference corrosion of section

Condition of Section	Eq. H-1 (2 years)	Multipliers* Eq. H-1	Amount of Thickness loss per side, mils
Good condition	$34*2^{0.65}$=53.35/25.4	2.10 * 2.75 * 1.0	5.77 = 6
Slight corrosion	$65*2^{0.5}$=91.92/25.4	3.625 * 2.75 * 1.7	16.9 = 17
Heavy corrosion	$80*2^{0.8}$= 139.29/25.4	5.48 * 2.75 * 2.0	30.16= 30

Table 2-6 Summary of % reduction in section modulus (2 years)

Condition of Section	% reduction in Section modulus (mean, 2-year period)
Good condition	1.8
Slight corrosion	5.0
Heavy corrosion	9.0

The penalty to the section modulus for the remaining section is reflected in a bias term (i.e., the ratio of mean to nominal values for a parameter). Variation of losses at specimens observed during ASTM testing were quantified as coefficients of variation, COVs, and approximated in ϕ factors using a simplified formulation. The values implemented in NCHRP 301 are summarized in Table 2.7. Note that a bias of 1.1 corresponds to the design assumption for new construction at the time. The flowchart in Figure 2.3 summarizes the procedure proposed in NCHRP 301 to account for deterioration.

Table 2-7 Summary of bias and COV for different section condition

	Bias	COV
New condition, steel member	1.10	12%
Partially corroded with some section loss	1.05	16%
Severe corrosion with considerable loss of section	1.00	20%

Moses revisited the condition factor in NCHRP 454 (Moses, 2001). In that report, Moses clarified that adjustments to sound material area should be decoupled from the increased uncertainty associated with deteriorated conditions. Load ratings should be performed using the sound material area at the time of inspection. Accordingly, the condition factors presented in NCHRP 454 are slightly higher than those in NCHRP 301. The values in NCHRP 454 have been incorporated into the MBE.

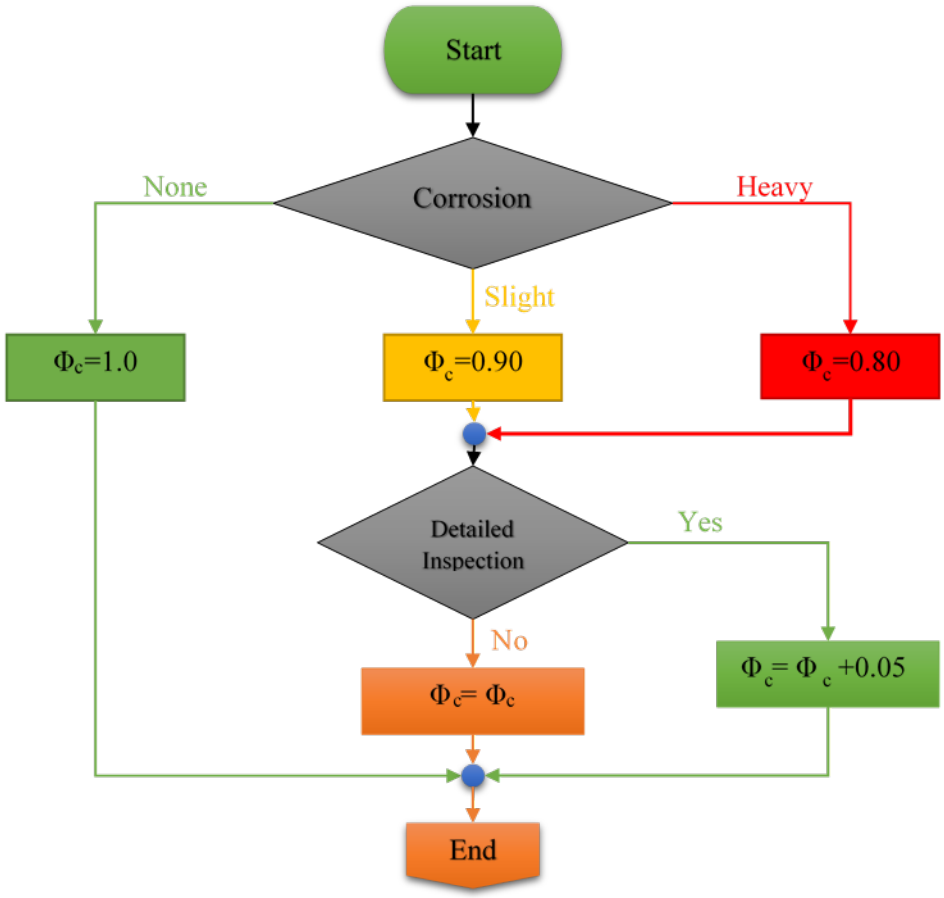

Figure 2.3 Flowchart for selecting resistance factor according to NCHRP 301

2.4 Steel Bridge Reliability with Deterioration

Kayser and Nowak (1989a, 1989b) discussed the impact of deterioration on long-term performance of steel girder bridges. Aspects of the work appear to be unrepresentative of typical bridges. In Kayser and Nowak (1989a), for example, the authors provide a figure illustrating the variation in moment capacity with flange thickness loss. The figure appears to indicate that a W30x99 noncomposite girder with a flange loss of less than 0.03 inches will incur a loss in capacity of approximately 30%. The general trends of plots appear reasonable, such as shear

capacity transitioning from a yielding to a buckling mechanism, but the exact values may need to be carefully validated before considering implementation in present studies.

Kayser and Nowak indicated in both articles that shear could potentially control deteriorated steel girder bridge capacity, but this finding, too, seems unrealistic. In Kayser and Nowak (1989a), the paper culminates with example rating variations over time, governed by flexure, shear, and bearing with and without stiffeners present. Two cases are presented: a 12 m (40 ft) bridge, and a 18 m (60 ft) bridge. The paper found that flexure would continuously control the rating for the 18 m bridge over the 50 year life of the structure, if stiffeners were provided. However, the authors found that the 12 m bridge would be governed by shear after about 15 years of deteriorating service. The initial load ratings for the 12 m bridge were similar, at about 1.8 in flexure and 2.0 in shear. The 18 m bridge, on the other hand, had initial load ratings of about 1.5 in flexure and 3.0 in shear, which would seem to be a more typical comparative relationship for a steel girder system than the nearly identical 12 m bridge ratings. While the theoretical frameworks discussed by the authors hold merit, the findings themselves are not of particular use to the present study.

Wang (2010) described a framework, developed through a PhD program under the supervision of Dr. Bruce Ellingwood, to explicitly incorporate reliability in highway bridge condition assessment. The proposed framework is arranged into three levels. The first level is similar to that discussed in this report, where relatively coarse information is mapped into LRFR condition factors. The second and third levels incorporate more detailed bridge-specific conditions, such as material strength and load patterns, with component-level (second tier) and system-level (third tier) refinement. In the first level, the research traces coarse SI&A superstructure condition rating for concrete bridges to phenomenological deterioration models

(estimated reinforcing section loss), also accounting for projected future losses. As the SI&A rating fell, the expected value of capacity reduced, and the capacity uncertainty increased. The variation of probabilistic capacity metrics was mapped through reliability analyses to identify optimum condition factors, as summarized in Table 2.8.

Table 2-8 Proposed condition factors by Wang (2010)

Structural Condition Rating (SI&A)	ϕ_c
≥ 8	1.0
7	0.95
6	0.85
5	0.75
≤ 4	0.70

Chapter 3: Overview of Methodology

Condition factors (ϕ_c) in LRFR account for increased capacity uncertainty associated with deterioration. This study includes the uncertainties in capacity associated with the severity and location of deterioration along a girder. These uncertainties are primarily influenced by the level of detail available from inspections.

3.1 Condition States and ϕ_c

The MBE recognizes three member condition states for deteriorated elements (e.g., girders). Table 3.1 lists the three structural conditions of the member and their corresponding ϕ_c reduction according to the MBE. The MBE does not provide definitions for these structural condition states. Rather, the MBEI should be consulted to assess conditions based on defects observed during field inspections.

Table 3-1 MBE structural condition of member and corresponding ϕ_c values

Structural Condition of Member	ϕ_c
Good or Satisfactory	1.00
Fair	0.95
Poor	0.85

The MBEI provides guidance to assess and classify severity for multiple defects at each of hundreds of elements. This research focuses on corrosion of steel girders, element #107 in the MBEI. MBEI condition state criteria are ambiguous and subjective. For example, condition state 4 is simply characterized by, “the condition warrants a structural review.” As an alternative to using MBEI condition states, the MBE commentary suggests the approximate correlation shown in Table 3.2, using SI&A reported superstructure condition ratings. A discussion of how

deterioration severity ambiguity was addressed in this research is found in a later section (refer to 5.3 Uncertainty due to Range of Section Loss in each Condition State).

Table 3-2 MBE condition state rating Table 6A.4.2.3-1

Superstructure Condition Rating (SI & A Item 59)	Equivalent Member Structural Condition
6 or higher	Good or Satisfactory
5	Fair
4 or lower	Poor

A review of bridge inspection reports found that the availability of detailed information varied significantly across the inventory. For example, county bridges generally had fewer details compared to state bridges inspected by NDOR personnel. Consequently, this study proposes multiple approaches to assign ϕ_c, as appropriate, to the available detail from inspections. The approaches are listed below with the corresponding appropriate level of detail available from inspections.

- Approach 1: Only the worst condition state in the girder is known.
- Approach 2: All condition states present in the girder and the corresponding total length of girder segments classified in each condition state are known.
- Approach 3: All condition states present in the girder and the corresponding length of girder segments classified in each condition state along with the location, are known.
- Special Approach: Deterioration profile (i.e., % section loss) along the span is known.

3.1.1 Inspection Methods, Policies, and Procedures in use by NDOR

The NDOR Bridge Inspection Program (BIP) Manual includes policies, procedures, required forms, reference documents, supplemental guidance and memos to guide inspectors in their duties. This document has detailed instructions on bridge inspection procedures and the qualifications as well as the certifications of the inspectors to perform the inspections. The manual also includes instructions for the structure of the bridge inspection team in Nebraska, quality assurance procedure for inspection, and bridge data to be submitted and reported to FHWA and NDOR. Since 2014, NDOR has moved to the Element Inspection method for rating their bridges because it provides "a more detailed picture of the health of their bridges than the broad NBI condition."

NDOR inspectors fill out a "Field Inspection Form" for each inspected bridge. The form requires general information about the bridge, including the structure number, location, year built, year reconstructed, and the geolocation. The traditional SI&A rating for the deck, superstructure, substructure, and culvert are also assessed and reported to the NBI database. Additionally, element level inspection data is recorded for various deterioration mechanisms and element types.

The form typically reports element level data as the portion of each element type at a bridge (e.g., total length of steel girders) categorized in each condition state (Good, Fair, Poor, Severe) for each applicable deterioration mechanism (e.g., corrosion). Locations of deteriorated conditions and measurements of section loss or remaining section are not generally available, unless deterioration is particularly severe. However, it is common practice (particularly for state bridges inspected by NDOR personnel) to take pictures during the inspection.

3.2 Bridge Surveying and Describing and Profiling the Deterioration

3.2.1 Deterioration Patterns

A review of the literature, together with pictures available from NDOR inspections, indicated that two deterioration profiles were appropriate for this study. One of the predominant corrosion patterns for simple span bridges is corrosion in the bottom flange and the bottom region of the web, with deterioration extending the full girder depth at supports below deck joints. Figure 3.1 shows examples of deterioration near the support, in contrast to Figure 3.2, which shows deterioration concentrated along the bottom flange and the bottom portion of the web.

For the second prevalent corrosion pattern, the full height of the girder had experienced corrosion at particular locations along the span. This type of corrosion, typically corresponds to deck cracking, allowing the leakage of electrolytes (water and deicing salt) similar to support conditions. Examples of this deterioration profile are provided in Figure 3.3 and Figure 3.4.

Figure 3.1 Deterioration pattern at girder ends

Figure 3.2 Bottom flange deterioration along the girder

Figure 3.3 Deterioration pattern where entire section of girder is deteriorated

Figure 3.4 Entire girder section deteriorated below the cracked slab

3.2.2 Girder Deterioration Profile Models

Nowak noted that steel girder corrosion from traffic spray accumulation commonly occurs along the top surface of girder bottom flanges and the bottom portion of the web. As noted previously, corrosion often extends over the entire web height near the support due to deck leakage (Kayser & Nowak, 1989a). At the mid-span, corrosion of the web reaches approximately ¼ of the web height. Figure 3.5 shows the corrosion pattern across a girder cross-section as developed by Czarnecki and Nowak (Czarnecki & Nowak, 2008), and a typical corrosion pattern found at steel girder bridges is shown in Figure 3.6.

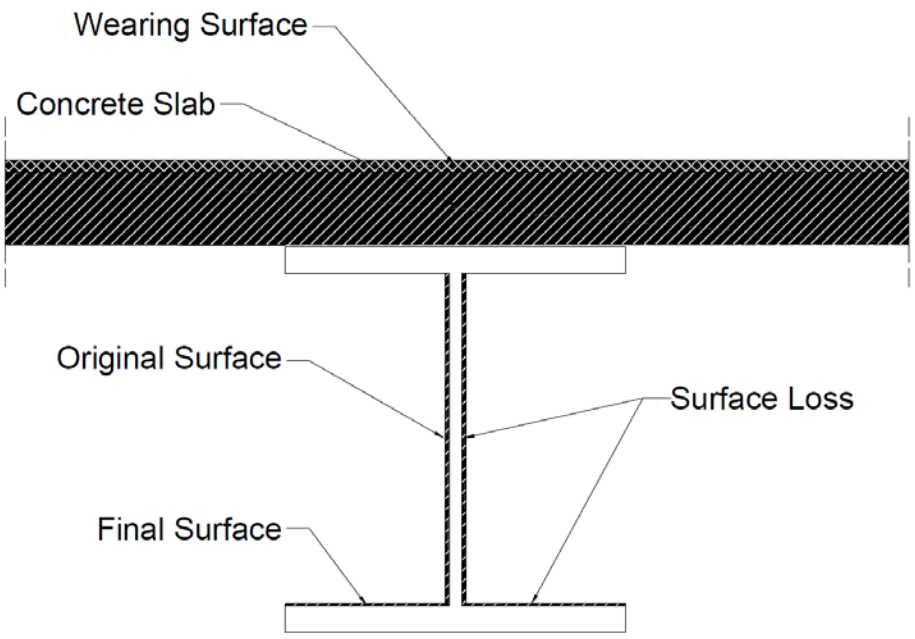

Figure 3.5 Corrosion of a steel girder bridge

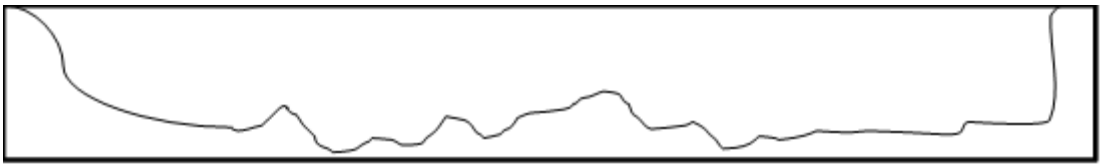

Figure 3.6 Typical corrosion pattern in a steel girder

Kayser and Nowak modeled deterioration along the entire web and the bottom flange at girder ends. Elsewhere along the span, corrosion was assumed at the bottom 1/4th of the web and the bottom flange. In this deterioration profile, the height of the deteriorated web decreases until it reaches 1/4th of the web height at 1/10th of the length and the deteriorated web height remains constant throughout the rest of the span. This type of profile is typically observed for bridges with decks in Good condition without leakage. Figure 3.7 and Figure 3.8 shows the deterioration profile in elevation and deteriorated cross-sections, respectively. This type of deterioration will be referred to as "girder deterioration profile 1," or "GP1," in this report.

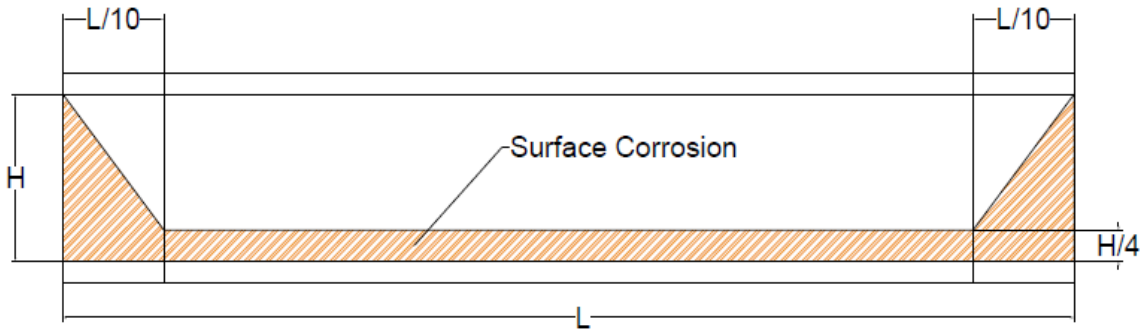

Figure 3.7 Deterioration profile "GP1"

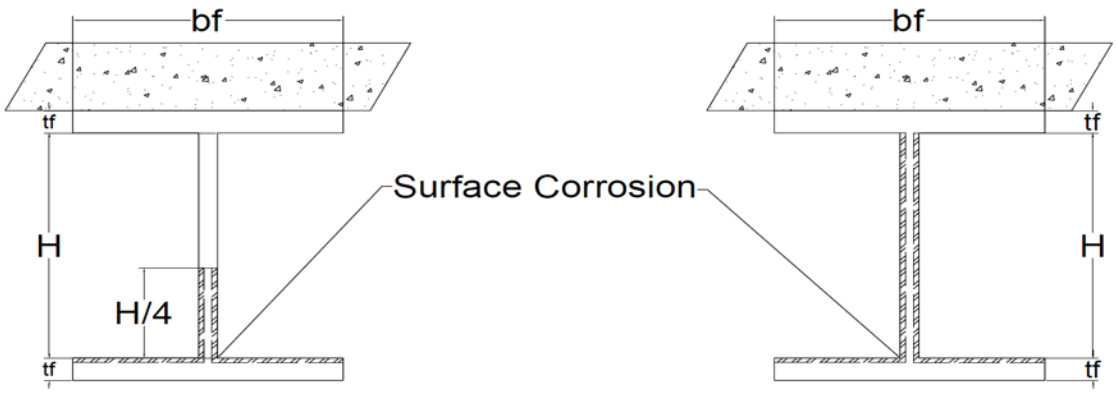

Figure 3.8 Section deterioration "GP 1"

The second predominant corrosion pattern exhibits corrosion along the full height of the section. In this deterioration profile, the entire girder depth is deteriorated, including both the flanges and the web. This profile is assumed to occur randomly along the span, caused by the leakage of deicing salt and water through damaged or cracked deck. Figure 3.9 shows this type of deterioration profile and the section profile. This type of deterioration will be referred to as "girder deterioration profile 2," or "GP2," in this report.

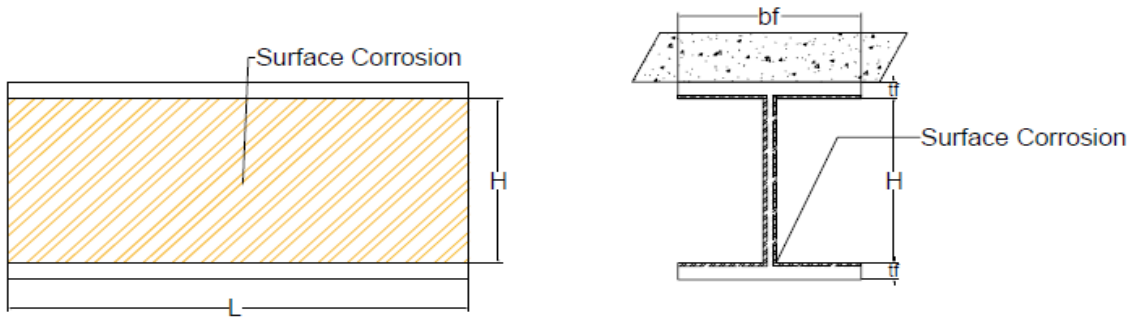

Figure 3.9 Entire web deteriorated along the span "GP 2"

Chapter 4: Reliability Analysis

Reliability analyses were performed to determine condition factors, ϕ_C, using the Rackwitz-Fiessler method. Rackwitz-Fiessler is used for this study because it can account for non-normal random variables. It uses the "equivalent normal" value for each non-normal random variable. The mean, standard deviation, and probability distribution of all random parameters involved in the limit function are required. The mean and standard deviation of non-normally distributed random variables are converted to equivalent normal mean and standard deviation values. These equivalent values are used in the analysis on the failure surface described by g = 0, where g is a limit state function.

Reliability analysis is performed using the load rating equation shown below in Eq. (2) to describe the limit state surface. This equation contains the capacity, dead load from a wearing surface, dead load from components, any other permanent loads and a live load with impact. For this study, the wearing surface and permanent loads on the bridges were neglected. The dead load includes the slab and girder self-weight. The live load in the analysis is HL 93 truck, which includes an HS 20 truck load and a lane-load of 0.64 kip/ft.

The process of performing reliability analysis starts with the rating equation, along with defining the variables and their parameters.

$$Load\ Rating\ (LR) = \frac{\phi\phi_s\phi_C R_n - \gamma_{DC}(DC) - \gamma_{DW}(DW) \pm \gamma_P(P)}{\gamma_{LL}(LL + IM)} \quad (2)$$

Rearranging into a limit state format (i.e., g = capacity – demand):

$$g = \phi\phi_s\phi_C R_n - \gamma_{DC}(DC) - \gamma_{DW}(DW) \pm \gamma_P(P) - (LR) * \gamma_{LL}(LL + IM) \quad (3)$$

Where,

$\phi, \phi_s, and\ \phi_C = Resistance\ factors$

$R_n = Capacity\ of\ the\ girder$

$\gamma_{DC} and\ \gamma_{DW} = Dead\ load\ factor\ for\ component\ dead\ load\ and\ wearing\ surface$

$DC\ and\ DW = Dead\ load\ from\ the\ component\ and\ wearing\ surface$

$\gamma_P = Load\ factor\ for\ permanet\ loads$

$P = Permanent\ loads$

$\gamma_{LL} = Live\ load\ factor$

$LL = Live\ load$

$IM = Impact\ factor$

For this study, the following assumptions apply in Eq. (3):

- No permanent loads are considered (P=0)
- Wearing surface is neglected (DW =0)

The following parameters were selected to maintain consistency with the current LRFR method in the MBE:

- ϕ = 1.0 for flexure.
- ϕ_s = 1 for multi-girder bridges.
- IM (impact factor) = 1.33
- LL is calculated for an HL 93 truck for Inventory rating with a COV of 0.18 (Moses, 2001).

Additionally, the following modifications were introduced:

- LR and γ_{LL} were combined into a Γ_{LL} term
- $\phi^* \phi_s * \phi_c$ were combined into a Γ_{RN} term

The modified governing equation for the failure surface is:

$$g = \Gamma_{RN} * R_n - [\Gamma_{ll}(LL + IM) + \gamma_{DC}(DC)] \quad (4)$$

Where,

$\Gamma_{LL} = LR * \gamma_{LL}$

$\Gamma_{RN} = \phi\phi_s\phi_C$

$R_n = Plastic\ moment\ capacity\ of\ a\ girder$

Structural capacity is taken as the plastic moment capacity of the remaining sound section, and it is modeled as a normally distributed random variable. Dead load is the moment caused by an 8-inch slab and the self-weight of the girder. This study assumed that the variation in dead load did not change with the decreasing condition of the girder (Kayser & Nowak, 1989b). Consequently, dead load is modeled as a deterministic parameter, with uncertainty accounted for in the typical LRFR dead load factor. This assumption was applied to avoid requiring changes to dead load factors from those commonly used in LRFR. Live load is the moment caused by the HL93 truck, and has a lognormal distribution with a COV of 0.18 and a bias of 1.00, which is consistent with the AASHTO LRFD design specification (Moses, 2001).

Design points for the moment capacity and the live load are determined during the reliability analyses to correspond to a target reliability. Γ_{LL} and Γ_{RN} are the ratios between the design point and mean values for live load and capacity, respectively. LR and ϕ_c can then be extracted from Γ_{LL} and Γ_{RN} using known γ_{LL}, ϕ, and ϕ_s.

All the load parameters are specific to a bridge. The mean load on the bridge depends on the length and the configuration of the bridge. They are independent of the condition state of the girder. Live load, impact, and dead load are constant for all condition states, as they are

independent of the deterioration in the girder. The live load along the span is equal to the moment envelope generated by an HL93 truck. Girder line analysis uses the girder distribution factor to find the appropriate proportion of the live load distributed to the girder. The dead load along the span is the moment generated by a uniformly distributed load equal to the weight of the concrete slab and the girder.

Capacity is dependent on the remaining sound material of the girder, and so changes with deterioration. The mean and standard deviation for capacity in each condition state is probabilistically characterized as discussed in the following chapters. The bias for capacity is taken as 1.00 because adjustments from mean to nominal capacity related to typical fabrication, material, and professional biases are assumed to be embedded in LRFD together with the ϕ factor. Girder plastic moment capacity is the governing limit state, and is calculated according to AASHTO LRFD for a composite, compact section.

The limit state function is satisfied by $g \geq 0$, where g is defined in Eq. (4). The procedure to conduct reliability analyses with the Rackwitz-Fiessler method is outlined below.

1. An initial design point for capacity is set to the mean capacity of the girder.
2. The live load corresponding to the capacity on the limit state surface can be calculated by solving the equation below.

$$LL = R_n - \gamma_{DC}(DC) \tag{5}$$

3. Equivalent normal parameters are determined for all non-normal parameters. The live load has a lognormal distribution with a COV of 0.18 and a bias of 1.00 (Moses, 2001), and the capacity, which is binned together for each condition state (as discussed later in this report), is assumed to be normally distributed.

4. The mean and standard deviation of the normally distributed variables are used to find the column vector of sensitivities, {G}, containing the partial derivatives of g with respect to the reduced variables, in this case, LL and Rn.

$$\{G\} = \begin{cases} -\dfrac{\partial g}{\partial Rn} \\ -\dfrac{\partial g}{\partial LL} \end{cases} \tag{6}$$

5. The column vector {α} is then determined using {G}.

$$\alpha = \frac{[\rho]\{G\}}{\sqrt{\{G\}^T[\rho]\{G\}}} \tag{7}$$

The coefficient of correlation [ρ] is a 2 X 2 identity matrix for a reliability analysis with two uncorrelated variables (applied live load and flexural capacity).

6. A new design point in reduced variates for n-1 variables (where, for this study, n = 2, so n-1 = 1) is determined using:

$$z^*_{RN} = \alpha_{RN}\beta_{target} \tag{8}$$

7. Corresponding design point values (x^*_{RN}) in original coordinates for the n-1 values in step 6 are determined from:

$$x^*_{RN} = \mu_{X^e_{RN}} + z^*_{RN}\sigma_{x^e_{RN}} \tag{9}$$

8. Determine the values of the live load using the equation g = 0 and recalibrate the mean of capacity ($\mu_{x_{RN}}$) using the following equation.

$$\mu_{x_{RN}} = \frac{x_{RN}^*}{1 + \alpha_{RN}\beta V_{X_{RN}}} \tag{10}$$

9. Repeat steps 3 through 8 until {α} converges
10. Once convergence is achieved, calculate the design factors (γ_i) using

$$\gamma_i = \frac{x_i^*}{\mu_{x_i}} \tag{11}$$

The terms used in the foregoing procedure reflect those presented in Nowak and Collins (2013). Referring back to the original limit state function developed for this study, γ_{LL} in Eq. (11) corresponds to Γ_{LL} in Eq. (4) and γ_{RN} in Eq. (11) corresponds to Γ_{RN} in Eq. (4). To find Load Rating (LR):

$$LR = \frac{\Gamma_{LL}}{\gamma_{LL}} \tag{12}$$

Note that the γ_{LL} used in Eq. (12) is taken from LRFR. It is not the value obtained in Eq. (11). Similarly, the condition factor, ϕ_c, is found from:

$$\phi_C = \frac{\Gamma_{RN}}{\phi\phi_s} \tag{13}$$

This process is used multiple times to generate ϕ_c values in this study (Nowak S. & Collins R., 2013). All the uncertainties that are accounted for by the ϕ_c are discussed in detail in Chapter 5: Uncertainty Contributions to Condition Factors.

Chapter 5: Uncertainty Contributions to Condition Factors

The factor ϕ_c accounts for uncertainties associated with the current deteriorated condition of the girder. These uncertainties include the change in the variation of measurement within sections (section 5.1 Uncertainties in Section Deterioration), possible future corrosion (section 5.2 Future Corrosion), the severity of section loss associated with condition states (section 5.3 Uncertainty due to Range of Section Loss in each Condition State) and the location of section loss along the span (section 5.4 Uncertainty in the Location of the Deterioration). There are three girder condition states considered in this study (Good, Fair, Poor), and ranges of the severities (percentage section loss) are combined within each condition state. Therefore, a new set of uncertainties associated with the exact percentage loss in the girder emerges. This uncertainty is also accounted for by the ϕ_c.

5.1 Uncertainties in Section Deterioration

Corrosion along a deteriorated section is non-uniform and causes variation in flange and web thicknesses, increasing uncertainty in the capacity of the girder. A relationship between measured percentage loss and the variation in actual thickness across a cross-section should be included in the reliability analysis when determining ϕ_c. No prior studies were found documenting the variation in section across a cross-section. Therefore, measurements were taken in the field for various girders to estimate this uncertainty.

5.1.2 Measurement in the Field

NDOR provided a list of 60 steel girder bridges near Lincoln, Nebraska, along with recent inspection reports. The reports helped identify the worst condition state present in the girder. The sample included a diverse range of bridges with all four condition states present.

The bridges were categorized into four groups depending on the worst condition state present in the bridge. Out of the 60 bridges, 4 bridges had condition state 4 as their worst

condition state in the inspection report, 28 bridges had condition state 3, 24 bridges had condition state 2, and 4 bridges had condition state 1. Table 5.1 lists 9 bridges that were visited and at which measurements were taken.

Table 5-1 List of bridges visited, their condition state and max % loss summary

Structure Number	Worst CS classification	Max % loss
S006 28494	**CS 3**	**3 %**
S033 01026	**CS 3**	**3 %**
S006 30574	**CS 1**	**1 %**
S006 28424	**CS 3**	**3 %**
S077 06205L	**CS 1**	**1 %**
S077 06205R	**CS 3**	**1 %**
S006 32007	**CS 3**	**14 %**
S136 14969	**CS 3**	**8 %**
S015 03097	**CS 3**	**8 %**

Measurements were taken in three different preparation states: deteriorated, brushed and ground. A location along the bottom flange was selected (see Figure 5.1) for each measured girder, and 10 sets of measurements were taken at each side of the flange (see Figure 5.2 and Figure 5.3). Measurements were taken within a 1 inch strip measured along the girder span at each selected location.

The measurements were repeated for each preparation state. First, measurements were taken without any modification to the surface except for removal of loose debris by hand. The location was cleaned using a steel brush, and measurements were retaken. Lastly, the location was cleaned with a power grinder, and measurements were taken again. The same girder was also measured at an undeteriorated section along the span to establish a baseline for comparison at the deteriorated section.

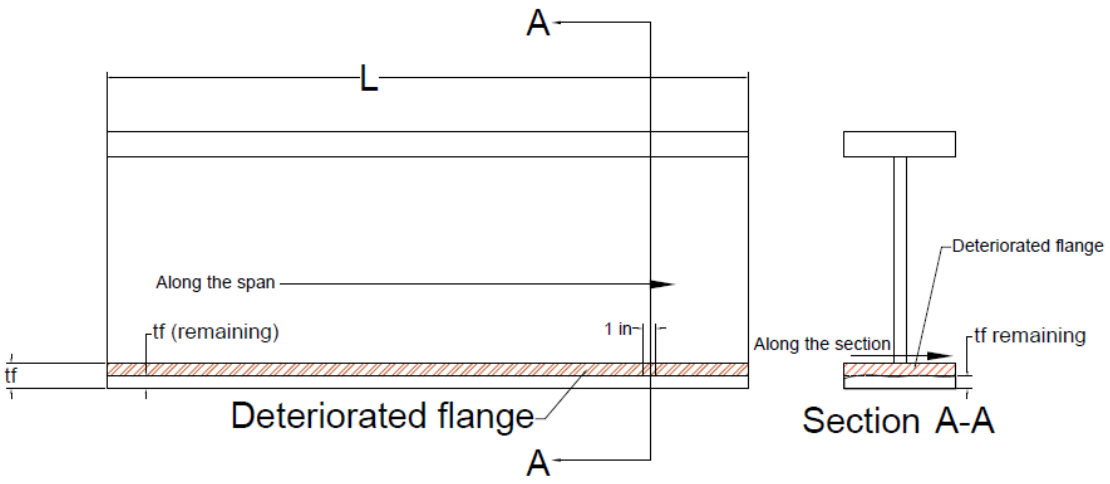

Figure 5.1 Section deterioration

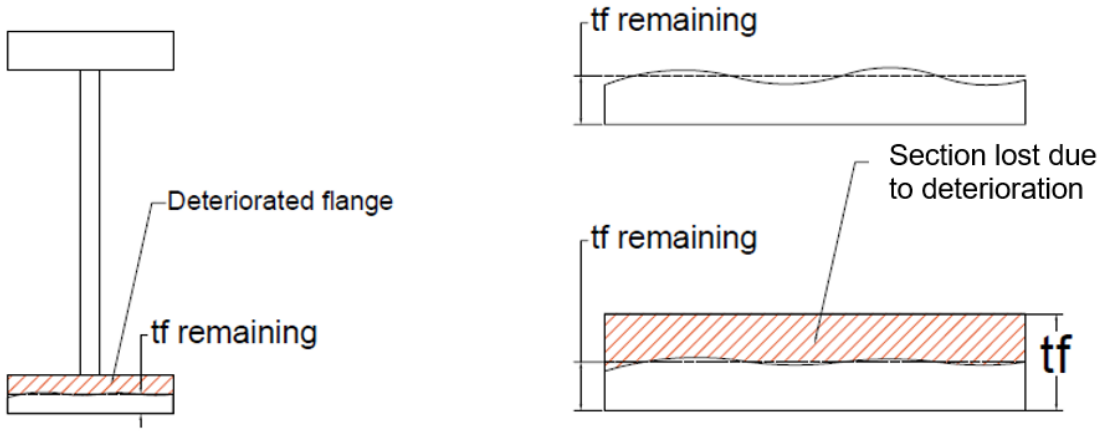

Figure 5.2 Variation of the flange thickness along the section

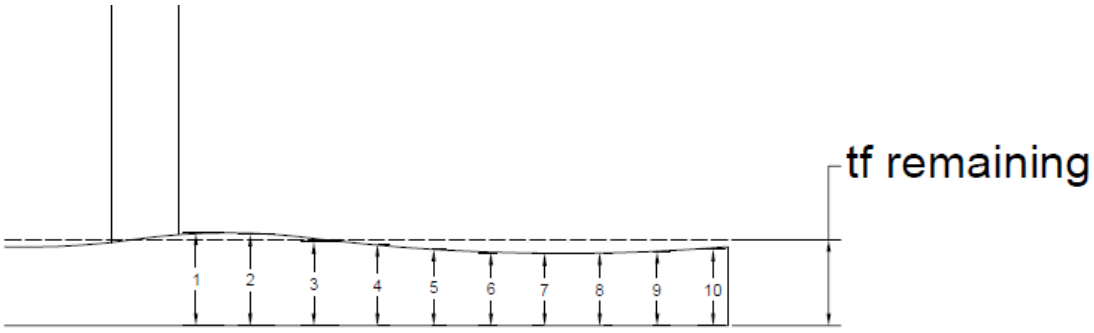

Figure 5.3 Sample location of measurement taken along the bottom flange

Mean and variation for percentage loss were calculated using the measurements from the undeteriorated section and the three states of measurements along the sections. The MBE recommends removing rust with a steel brush. However, grinding was required to reach sound material, because the steel brush did not remove all of the rust. ASTM G103 cautions against grinding to avoid loss of sound material. Mechanical girding was the only option for removing all of the rust from the steel because other procedures, such as chemical or electrolysis techniques, which were not feasible in the field. The grinding process was carefully performed to minimize removal of sound material. A material that is softer than steel was used for grinding, and the girding was stopped soon after sparks appeared.

All measurements were taken using a deep throat micrometer (see Figure 5.4) because of its high precision and the ability to take measurements at multiple locations across a flange with varying remaining thickness (calipers can only measure the thickest area of a deteriorated flange).

Figure 5.4 Wide mouth caliper used for measurement of the flange

Excel was used to record and analyze all measurements. The Excel sheet recorded information including the structure number and location of the bridge, the length of each condition state, and the total length of the girders. See Figure 5.5 for an example of the measurement sheet. The mean, standard deviation, COV, median, quartiles and outlier boundaries were calculated in the excel sheet. Any measurement that is beyond the outlier boundaries were highlighted to receive attention later during analysis.

The COV and the mean loss are the two most important parameters. Percentage section loss is determined using the mean values of the undeteriorated section and the ground section. The difference between the two divided by the mean undeteriorated value is the percentage loss. COVs were calculated by dividing standard deviations by mean values. The COV of the ground measurement is then linked to the percentage loss for measurement used in reliability analyses. A list of all the percentage losses and the corresponding COVs are shown below in Table 5.2.

Structure Number		S006 28424			
Date of Inspection		7/20/2016			
Location		3N DORCHESTER at JOHNSON CREEK			
Total length [ft.]		450			
Condition State		CS 1	CS 2	CS 3	CS 4
Length [ft.]		440	0	10	0
	[mm]	[mm]	[mm]	[mm]	[mm]
Reading	No deterioration	After Brushing	After Grinding	After Brushing	After Grinding
1	38.68	37.08	38.8	38.39	37.04
2	38.46	36.24	37.91	37.92	37.27
3	38.84	36.67	37.71	38.50	37.33
4	38.74	36.98	37.81	38.57	37.64
5	38.51	37.68	37.43	38.30	37.70
6	38.62	37.64	37.09	38.41	38.01
7	38.49	37.95	37.41	38.25	38.11
8	38.82	37.8	37.46	37.87	37.92
9	38.8	38.01	36.87	37.73	37.76
10	38.59	38.00	36.88	37.64	37.61
Mean	38.66	37.41	37.54	38.16	37.64
Standard Deviation	0.142	0.6225	0.5724	0.3200	0.3237
% loss	0%	3%	3%	1%	3%
COV	0.0037	0.0166	0.0152	0.0084	0.0086
median	38.65	37.66	37.45	38.275	37.67
1st quartile	38.53	37.01	37.17	37.8825	37.40
3rd quartile	38.78	37.91	37.79	38.405	37.88
lower fence	38.15	35.64	36.25	37.09875	36.68
upper fence	39.17	39.27	38.71	39.18875	38.60

Figure 5.5 Example field measurement sheet along with the calculated loss and COV

The COVs and the percentage losses were plotted to examine the relationship between the percentage loss and the COV. No clear trend was found. A linear fitting had a poor R^2 of only 0.65 (see **Figure 5.6**). A step function approach to assign COVs to percentage losses was used, where the larger COV between the COV for the considered section percentage loss and the

COV that was assigned to a lower percentage section loss is selected. For example, the COV for a 4% loss is 0.028 and the COV for a 5% loss is 0.011; the COV used for a 5% loss is 0.028 because that is the maximum COV for all values less than or equal to a 5% loss. The solid line (red) in Figure 5.6 shows this approach. A summary of the percentage section loss and the corresponding COV is shown in Table 5.3. The maximum COV is carried forward constantly for section loss greater than the maximum measured (14%). This COV is incorporated in uncertainties considered during reliability analyses (see section 6.1.1 Quantifying Uncertainty in Approach 1).

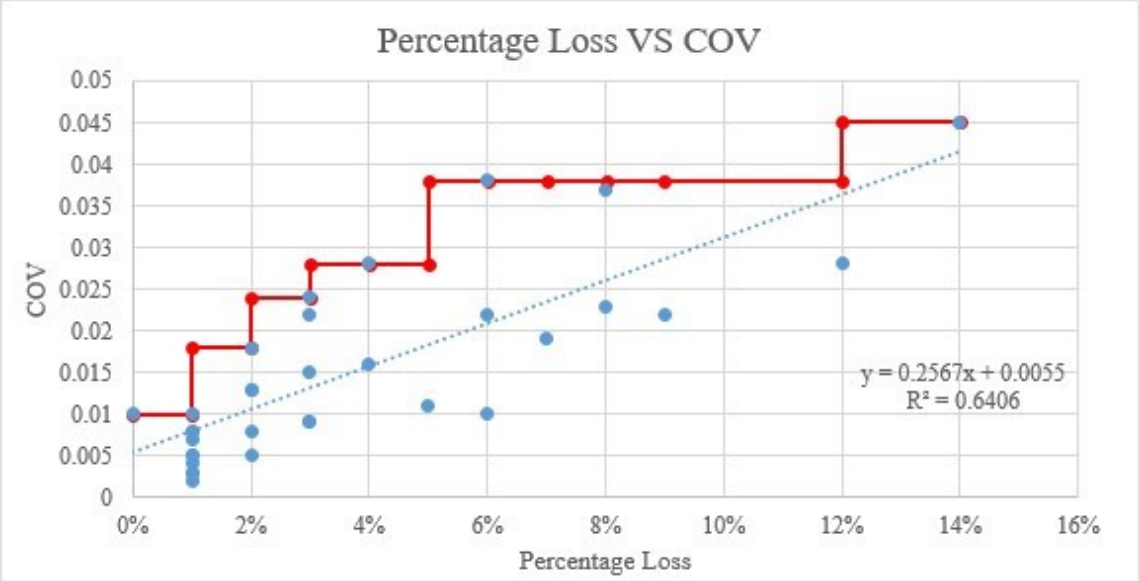

Figure 5.6 Percentage loss VS COV

Table 5-2 Summary of % loss and COV of bridges after grinding

Structure number	% loss	COV
S077 06205R	0%	0.01
S006 28494	1%	0.005
S033 01026	1%	0.008
S136 14969	1%	0.003
S077 06205R	1%	0.008
S006 30574	1%	0.003
S006 28494	1%	0.002
S077 06205L	1%	0.007
S077 06205R	1%	0.010
S006 28424	1%	0.005
S077 06205R	1%	0.004
S006 28494	2%	0.008
S006 28494	2%	0.013
S033 01026	2%	0.013
S033 01026	2%	0.018
S006 28424	2%	0.005
S006 28424	3%	0.009
S136 14969	3%	0.024
S 015 03097	3%	0.022
S006 28424	3%	0.015
S033 01026	3%	0.009
S136 14969	4%	0.028
S 015 03097	4%	0.016
S 015 03097	5%	0.011
S 015 03097	6%	0.022
S136 14969	6%	0.038
S 015 03097	6%	0.010
S006 32008	7%	0.019
S 015 03097	8%	0.023
S136 14969	8%	0.037
S006 32007	9%	0.022
S006 32007	12%	0.028
S006 32007	14%	0.045

Table 5-3 Summary of max COV for all percentage loss

Percentage Loss	Max COV
0	**0.010**
1	**0.010**
2	**0.018**
3	**0.024**
4	**0.028**
5	**0.028**
6	**0.038**
7	**0.038**
8	**0.038**
9	**0.038**
12	**0.038**
≥14	**0.045**

5.2 Future Corrosion

Future deterioration (between inspections) is considered in the reliability analyses using a bias (λ). Similar to NCHRP 301, Komp's corrosion model, including modifications for the presence of deicing salts and sheltered condition, is used to account for future corrosion loss. This model makes predictions based on the material and the environment. There are three environments and two types of steel in Komp's model, which results in a total of six different predictions for future corrosion. These modifications are used to account for the influence of the environment and other chemicals, and to predict the corrosion rate of bridges.

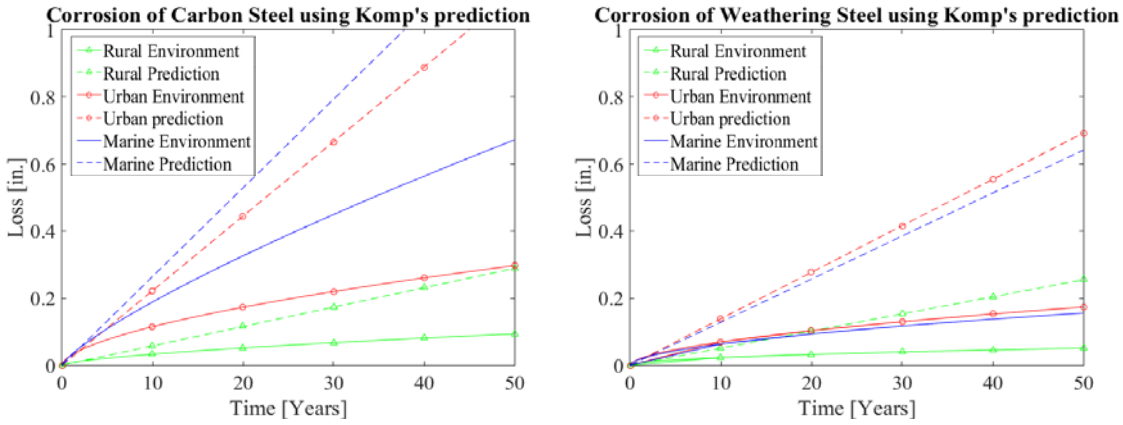

Figure 5.7 Prediction of future corrosion

Komp's model is an asymptotic function, therefore the rate of corrosion decreases in time, but a secant rate of the initial 2 years is conservatively used for the study. Corrosion losses for various materials and environments are shown in Figure 5.7. The Komp predictions are shown as solid lines, and the secant rates are shown as dashed lines. The projected girder moment capacity, accounting for future corrosion, is taken as the nominal value and the capacity at the time of inspection is taken as the mean in reliability analyses. The ratio between the mean and the nominal is the bias (λ). Bias (λ) for this research is shown in Eq. (14). The proposed ϕ_c values are calibrated for carbon steel in a rural environment because this was the most prevalent case in Nebraska. Other environments and type of steel can be obtained by applying a multiplier to the ϕ_c for carbon steel in rural environments.

$$\lambda = \frac{\mu}{d} = \frac{\mu_{RN}}{\mu_{RN,CR}} \tag{14}$$

Where,

$\mu = Mean\ in\ reliability\ analyses$

$d = Nominal\ in\ reliability\ analyses$

$\mu_{RN} = Mean\ plastic\ moment\ capacity\ of\ the\ girder\ at\ inspection$

$\mu_{RN,CR} = Future\ moment\ capacity\ after\ corrosion\ (carbon\ steel, rural\ env.)$

Alternate materials and environments can be assigned ϕ_c values by scaling the value obtained for carbon steel in a rural environment. In Eq. (15), the base ϕ_c that accounts for future deterioration of carbon steel in rural environment is calculated using the bias in Eq. (14). Similar ϕ_c for other types of steel and environments can be found (Eq. (16)). Eq. (17) through Eq. (20) illustrate that ϕ_c can be calibrated to alternate materials and environments using multipliers.

$$\phi_{C,CR} = \lambda \frac{R^*}{\mu_{RN}} = \frac{\mu_{RN}}{\mu_{RN,CR}} * \frac{R^*}{\mu_{RN}} = \frac{R^*}{\mu_{RN,CR}} \tag{15}$$

$$\text{Similarly, } \phi_{c,F} = \frac{R^*}{\mu_{RN,F}} \tag{16}$$

$$\phi_{c,F} = \frac{R^*}{\mu_{RN,F}} * \frac{\mu_{RN,CR}}{\mu_{RN,CR}} \tag{17}$$

$$\phi_{c,F} = \frac{R^*}{\mu_{RN,C}} * \frac{\mu_{RN,CR}}{\mu_{RN,F}} \tag{18}$$

$$\phi_{c,F} = \phi_{C,CR} * Multiplier \tag{19}$$

$$Multiplier = \frac{\mu_{RN,CR}}{\mu_{RN,F}} \tag{20}$$

Where,

$R^* = design\ value\ from\ reliabitlity\ analysis$

$\mu_{RN} = Mean\ plastic\ moment\ capacity\ of\ the\ girder\ at\ inspection$

$\mu_{RN,CR} = Moment\ capacity\ after\ corrosion\ (carbon\ steel\ in\ rural\ environment)$

$\phi_{C,CR} = Condition\ factor\ future\ corrosion\ (carbon\ steel\ in\ rural\ environment)$

$\phi_{c,F} = Conditon\ factor\ future\ corrosion\ (any\ steel\ in\ any\ environment)$

$\mu_{RN,F} = Average\ predicted\ moment\ capacity\ of\ the\ gider\ after\ corrosion$

$\mu_{RN,N} = \mu_{RN,CR}\ for\ carbon\ steel\ girder\ in\ rural\ environment$

A two-year estimation is used because inspections are typically performed every two years on all bridges. A conservative estimation of loss due to corrosion in two years can be used to estimate the maximum loss in section properties. This remaining section is used to calculate the capacity of the girder present at the next inspection cycle.

5.3 Uncertainty due to Range of Section Loss in each Condition State

Condition states in MBEI are not quantitatively correlated to section loss severity. For example, the bridge in Figure 5.8 might be documented in an MBEI-conformant inspection report to have 10% CS3, 20% CS2, and 70% CS1. This information provides little insight into the percentage loss that should be included in a load rating evaluation. Accordingly, ϕ_c should be calibrated to account for the uncertainty in available capacity for each and all applicable condition states. This study examines current inspection processes and proposes a range of section loss for each condition state, and an alternative range that would provide consistent reliability in load rating with the suggested ϕ_c values found in the MBE (AASHTO, 2014).

Figure 5.8 Bridge with multiple condition states

The variation in percentage loss in each condition state is assumed to be normally distributed for simplicity in the analysis. For future research, detailed surveying and measurement within each condition state could provide more insight into the distribution within each condition state. A range of admissible section loss severities needs to be specified for each condition state to quantify respective uncertainties.

5.3.1 Determining Range of Section Loss within each Condition State

Condition state, a term used in AASHTO's Manual for Bridge Element Inspection (MBEI), categorizes defects into 4 levels of severity (see Table 5.4), but the descriptions for each condition state are vague and subjective. The SI&A rating used in the NBI is used to broadly characterize the entire superstructure including all elements above the bearing of the bridge.

NDOR's BRIM includes a range of percentage losses in superstructure condition rating descriptions (see Table 5.5).

The description with percentage loss from the SI&A rating and the corresponding equivalent condition state (see Table 3.2) can be used to help choose a range for each condition state. Condition state 1 corresponds to "Good or Satisfactory" in the structural condition of a member, which has an SI&A superstructure condition rating of 6 or higher. Similarly, condition state 2 is "Fair" with an SI&A condition rating 5, condition state 3 is "Poor" with an SI&A condition rating of 4, and condition state 4 is "Severe" with an SI&A condition rating of 3 or lower. These correlations of MBEI condition states and SI&A superstructure ratings are compared to NDOR's condition rating descriptions in Table 5.6.

Table 5-4 Element #107 condition state definitions

Defect	Condition State			
	1	**2**	**3**	**4**
	Good	**Fair**	**Poor**	**Severe**
Corrosion	None	Freckled Rust. Corrosion of the steel has initiated	Section Loss is evident or pact rust is present but does not warrant structural review	The condition warrants a structural review to determine the effect on strength or serviceability of the element or bridge, OR a structural review has been completed and the defects impact strength or serviceability of the element or bridge.
Cracking	None	Cracks that has self-arrested or has been arrested with effective arrest holes, doubling plates, or similar.	Identified crack that is not arrested but does not warrant structural review.	
Connection	The connection is in place and functioning as intended.	Loose fasteners or pack rust without distortion is present but the connection is in place and functioning as intended	Missing bolts, rivets, or fasteners; broken welds; or pact rust with distortion but does not warrant a structural review.	
Distortion	None.	Distortion not requiring mitigation or mitigated distortion.	Distortion that requires mitigation that has not been addressed but does not warrant structural review.	
Damage	Not Applicable.	The element has impact damage. The specific damage caused by the impact has been captured in Condition State 2 under the appropriate material defect entry.	The element has impact damage. The specific damage caused by the impact has been captured in Condition State 3 under the appropriate material defect entry.	The element has impact damage. The specific damage caused by the impact has been captured in Condition State 3 under the appropriate material defect entry.

Table 5-5 Table C6A.4.2.3-1- from MBE: description of member condition

Code	Condition	Description
N	NOT APPLICABLE	For example, a culvert.
9	EXCELLENT CONDITION	No noticeable or noteworthy deficiencies that affect the condition of the structure.
8	VERY GOOD CONDITION	Bent steel or slight misalignment, not requiring repairs.
7	GOOD CONDITION	Heavy rust in localized areas without any section loss.
6	SATISFACTORY CONDITION	Initial section loss (heavy rust) in localized areas of structural steel members in non-critical stress areas
5	FAIR CONDITION	Substantial but not critical collision damage to structural support elements, steel girders, trusses, etc. Initial section loss (heavy rust) in localized areas of structural steel members in critical stress areas.
4	POOR CONDITION	Critical collision damage sustained to structural support elements. Precautionary measures such as traffic restrictions or temporary shoring may be needed. Significant section loss (heavy rust) of structural steel girder in critical stress areas. (More than 30% section loss).
3	SERIOUS CONDITION	Disintegration of or damage condition of a structural member which requires traffic restriction or shoring. Severe section loss (heavy rust) or structural steel member in critical stress areas requiring immediate repairs. (More than 50% loss of section).
2*	CRITICAL CONDITION	The need for repair or rehabilitation is urgent. Facility must be closed until the indicated repair is complete.
1*	IMMINENT FAILURE CONDITION	Facility is closed. Study should determine the feasibility for repair.
0*	FAILED CONDITION	Facility is closed and is beyond repair.

Table 5-6 Condition states with corresponding condition ratings and descriptions

Condition State	Condition of Member	Condition Rating	NDOR's Description
1	**Good**	**6 or higher**	Initial section loss in localized areas of structural steel members in non-critical stress areas.
2	**Fair**	**5**	Initial section loss (heavy rust) in localized areas of structural steel members in critical stress areas.
3	**Poor**	**4**	Significant section loss (heavy rust) of structural steel girder in critical stress areas. (More than 30% section loss).
4	**Severe**	**3 or lower**	Severe section loss (heavy rust) or structural steel member in critical stress areas requiring immediate repairs. (More than 50% loss of section).

NDOR's description for condition rating (see Table 5.5) has a Poor condition with more than 30% section loss. Similarly, the Severe condition is defined as having more than 50% loss of section, which can be inferred to limit condition state 3's section losses between 30% to 50%. The Fair condition does not have percentages bounds. A 10% lower limit for the Fair condition was chosen to keep the range of section loss equal to condition state 3. Condition state 2 was then assumed to range from 10% to 30%, and condition state 1 was assumed to range between 0 to 10%. Although having a 10% section loss is contrary to the description in the MBEI, it is closer to the Good condition description rating because the Good condition can have "initial section loss in localized areas of structural steel members in non-critical stress areas." This 10% is an upper limit and a conservative assumption. The MBE does not have a condition rating associated with condition state 4. An upper limit of 80% was arbitrarily selected. The range of section loss for each condition state is shown in Table 5.7.

Table 5-7 Condition state and a range of section loss in each condition state

Condition State	Range of section loss
1	<10%
2	10-30%
3	30-50%
4	50-80%

Preliminary reliability analyses were performed to determine an appropriate ϕ_c for each of these ranges of section loss. The ϕ_c for condition state 1 would be approximately 0.96; the ϕ_c for condition state 2 would be about 0.82, and the ϕ_c for condition state 3 would be around 0.68. These penalties seem inappropriately severe. For example, the ϕ_c value in MBE for a Fair condition element is proposed to be 0.95, compared the 0.82 obtained from preliminary analyses. In addition to the severe penalty, this approach is not consistent with MBEI inspection procedures. A new range consistent with Element Level Inspection was determined, as discussed in the following section.

5.3.2 Range Consistent with NDOR's Current Inspection Procedure

A range based on NDOR's current element inspection description for condition states, using the description in Table 5.4 Element #107 condition state definitions, is proposed in this section. Condition state 1 has no rust, indicating that the percentage loss for condition state 1 must be 0%. Condition state 2 is described as having some freckled rust with no measurable section loss. A maximum loss of 1% was selected based on this description. Condition state 3 is defined as having evident section loss. An arbitrary range between 1% to 50% section loss is assumed for condition state 3. Condition state 4, by definition, requires a structural review by an engineer. The lower limit of 50% was set for condition state 4 to correspond to the SI&A rating of 3 (serious condition, see Figure 5.5). The ranges are summarized in Table 5.8.

Table 5-8 Range of condition state consistent with Element Inspection

Condition State	Range of Section Loss
1	0%
2	0-1%
3	1-50%

Reliability analyses using the section loss ranges inferred from NDOR Element Inspection descriptions produced ϕ_c values inconsistent with those found in the MBE. For example, a girder with freckled rust is categorized as condition state 2, but MBE suggests a penalization of 5% (ϕ_c =0.95) to the girder capacity. "Freckled rust" was interpreted as negligible section loss, so the resulting condition factor from analysis was approximately 1.0 (rather than 0.95). All girders with measurable section loss are categorized into condition state 3. The wide range of section loss produced ϕ_c values significantly more severe for condition state 3 than proposed in MBE (ϕ_c = 0.85). Preliminary analyses for ϕ_c resulted in the values presented in Table 5.9 for the two girder deterioration profiles (GP).

Table 5-9 ϕ_c for two deterioration profiles using deterioration severity inferred from NDOR Element Inspection descriptions

	CS1	CS2	CS3
GP1	1.00	1.00	0.70
GP2	1.00	1.00	0.40

5.3.3 Calibrating the Range of Condition State to MBE Values

An alternative set of section loss ranges was calibrated to match the ϕ_c values suggested in the MBE, providing an alternative set of inspection guidelines for consideration by NDOR.

The bounds for section loss ranges were determined by trial and error for each condition state, starting from condition state 1 and progressing to more severely deteriorated conditions. All condition states were assumed mutually exclusive (i.e., no section loss can occur in more than one condition state). The reliability analyses presumed that the entire bridge exhibited uniform deterioration (i.e., no variation along the span). Reliability analyses implemented the Rackwitz-Fiessler method, as described previously. Capacity uncertainty a variation across a section and from the consideration of a range of section loss severities for the condition state under consideration. Future corrosion was reflected through bias in the reliability analyses.

Ranges of section loss were identified for each of the two deterioration profiles considered in this study, considering spans from 50 to 120 ft, as shown in Table 5.10. A range of section loss between 0 – 1% resulted in a ϕ_c of 0.99 for GP1, but only 0% loss was admissible for GP2 and would correspond to a ϕ_c of 0.98 (less than 1 to reflect potential future loss). Similarly, analyses indicated upper bounds for each span, deterioration profile (GP), and more severely deteriorated condition state (2 and 3).

The minimum of the upper bounds was selected as the “Final Range”, representing bounds on deterioration severity that will produce ϕ_c values no lower than those found in the MBE. These ranges of section loss are summarized for both deterioration profiles in Table 5.11. These ranges for each condition state were selected for use in this research.

Table 5-10 Range of section loss for condition state and their corresponding ϕ_c

	GP 1						
Length	**Shape**	**CS 1**	**CS 2**	**CS 3**	**ϕ_c 1**	**ϕ_c 2**	**ϕ_c 3**
50	**W30X99**	1%	7%	31%	0.99	0.94	0.85
60	**W33X118**	1%	7%	32%	0.99	0.94	0.85
70	**W36X135**	1%	7%	35%	0.99	0.94	0.85
80	**W40X167**	1%	7%	35%	0.99	0.94	0.85
90	**W36X194**	1%	7%	36%	0.99	0.95	0.85
100	**W40X215**	1%	7%	35%	0.99	0.95	0.85
110	**W44X230**	1%	7%	35%	0.99	0.95	0.85
120	**W44X262**	1%	7%	35%	0.99	0.95	0.85
	Final Range	1%	7%	31%			
	GP 2						
Length	**Shape**	**CS 1**	**CS 2**	**CS 3**	**ϕ_c 1**	**ϕ_c 2**	**ϕ_c 3**
50	**W30X99**	0%	5%	20%	0.98	0.95	0.84
60	**W30X116**	0%	5%	20%	0.98	0.95	0.85
70	**W33X130**	0%	5%	20%	0.98	0.95	0.85
80	**W36X150**	0%	5%	21%	0.98	0.95	0.85
90	**W36X182**	0%	7%	25%	0.99	0.95	0.85
100	**W33X201**	0%	7%	25%	0.99	0.95	0.85
110	**W40X211**	0%	5%	22%	0.99	0.95	0.85
120	**W40X249**	0%	10%	30%	0.99	0.95	0.85
	Final Range	0%	5%	20%			

Table 5-11 Range of section loss for condition states

Condition state		**Range of section loss**
GP 1	**1**	0-1%
	2	1-7%
	3	7-31%
	4	31-80%
GP 2	**1**	0%
	2	0-5%
	3	5-20%
	4	20-80%

5.4 Uncertainty in the Location of the Deterioration

5.4.1 Introduction

Load rating is a function of the structural demand induced by the load, which varies along the span. The critical load rating section for a new girder is near mid-span because the flexural demand by the load is maximum at the mid-span, and the capacity of a non-deteriorated girder is uniform throughout the span. Varying levels of section loss along the span results in non-uniform capacity, which could shift the critical load rating location.

For example, a hypothetical girder with a span length of 50 ft could have a section loss along the span as shown in Figure 5.9. The section loss of 50% at 12.5 ft (1/4 point of span) is the maximum loss present in the girder. Section loss for the hypothetical girder is minimum at the mid-span, at 20%. Load rating of the 50 ft W30X99 girder for an HL 93 truck is plotted in Figure 5.10. The load rating at the mid-span is 1.041, and the load rating at the location of maximum deterioration is 1.034. The critical load rating value of 0.9568, is located at 18.5 ft. along the span.

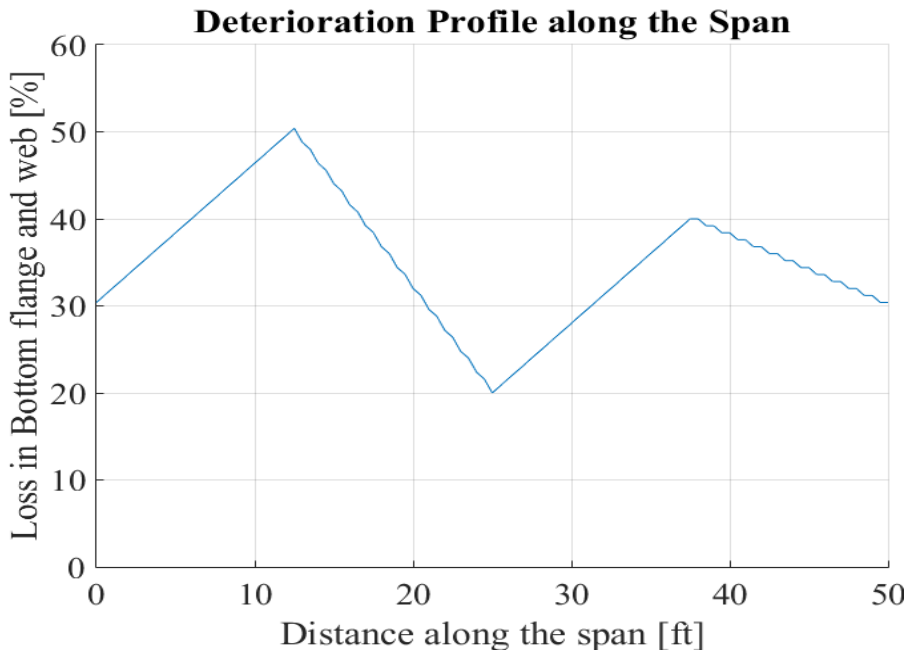

Figure 5.9 Example section loss profile along the span

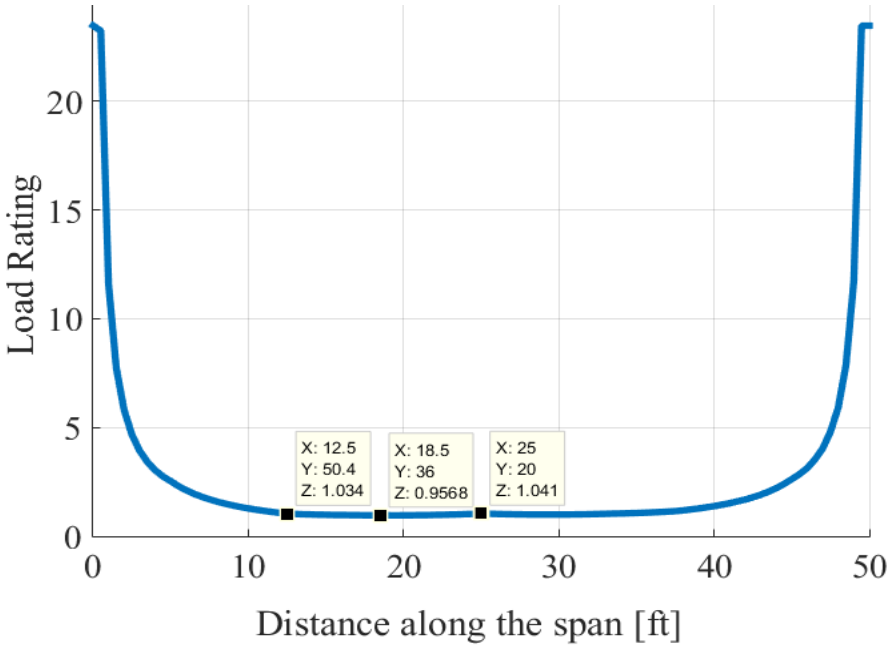

Figure 5.10 Load rating along the span for the section loss shown in Figure 5.9

5.4.2 Approaches to Determine ϕ_c Depending on Inspection Information

The critical load rating for the hypothetical bridge in the previous section can only be identified if inspection data provides detail similar to that shown in Figure 5.9. This research recognized that available inspection data varied across the inventory, and so four Approaches are proposed:

- only the worst condition state in the girder is known (Approach 1),
- all condition states present in the girder and the corresponding total length of girder segments classified in each condition state are known (Approach 2),
- all condition states present in the girder and the corresponding length of girder segments classified in each condition state along with the location is known (Approach 3), and
- detailed, exact deterioration profile along the span is known (Special Approach), similar to Figure 5.9.

The four Approaches are influenced by uncertainties differently, and therefore each must address uncertainties uniquely. Uncertainties for each approach were characterized and included in the reliability analyses as appropriate (refer to the following chapter for algorithmic details). Guidance is recommended for implementing ϕ_c's, based on the available inspection data and the corresponding appropriate approach.

For Approach 1, the only information known is the worst condition state in the girder. The uncertainties in this approach include the represented proportions of each condition state, the locations of condition states along spans, the severity of section loss (% loss) within each condition state, the variation of loss across the section, and the loss due to corrosion until the next inspection.

In Approach 2, the represented proportions (of total girder length) are known for each condition state. The uncertainties in this approach include the location of each condition state along the span, the severity of section loss (% loss) within each condition state, the variation of the loss across the section and the loss due to corrosion until the next inspection cycle.

In Approach 3, the represented proportions (of total girder length) and the locations of condition states along spans are known. The uncertainties in this approach include severity of section loss (% loss) within each condition state, the variation of loss across the section and loss due to corrosion until the next inspection.

The three common uncertainties on all of the approaches are severity of section loss (% loss) within each condition state, the variation of loss across the section, and projected future corrosion loss until the next inspection. Unknown exact % loss is addressed using a mean and standard deviation of capacity for all % loss integer increment cases in the condition state under consideration. For example, CS2 has a range between 1% and 5% loss; capacity mean and standard deviation within that range was calculated using Eqn. (21) and (22) respectively.

$$Average = \frac{\sum_{i=1}^{n} x_i}{n}, \tag{21}$$

$$standard\ deviation = \sqrt{\left(\frac{\sum((x - Average)^2)}{n-1}\right)} \tag{22}$$

Where,

x_i *is plastic moment capacity with* i^{th} % *loss in each condition state*

n *is number of* % *loss integer increments in each condition state.*

The calculated mean and standard deviation of the moment capacities were used in reliability analyses as a normally distributed random variable. The variation of deterioration across the section is accounted for as discussed in the following chapter, by combining dispersion measures using the square root of the sum of the squares (SRSS). The uncertainty due to possible future corrosion is likewise discussed in the following chapter.

The distribution of condition states (CS) along girder spans is treated by discretizing the girder length into 5% segments, as shown in Figure 5.11. Each line in the table below the beam represents a scenario when the total proportions of condition states are known along the span. For example, the next to last line (immediately above scenario 231) could be documented during an inspection as having 25% CS1 (5 green blocks of 5% each in the figure), 55% CS2 (11 yellow blocks), and 20% CS3 (4 red blocks). Alternatively, the report may only indicate that the bridge is in Poor condition (CS3), without providing insight into whether 5% or 100% of the bridge qualifies for this condition state.

The scenarios can be broadly characterized into CS groups when only the worst condition state is known (i.e., when Approach 1 must be used). The groupings are summarized in Figure 5.12. There are 3 CS groups: CS3 group includes all the scenarios with condition state 3, CS2 contains all the scenarios with condition state 2 but no condition state 3, and CS1 has the single scenario where the entire girder is in condition state 1.

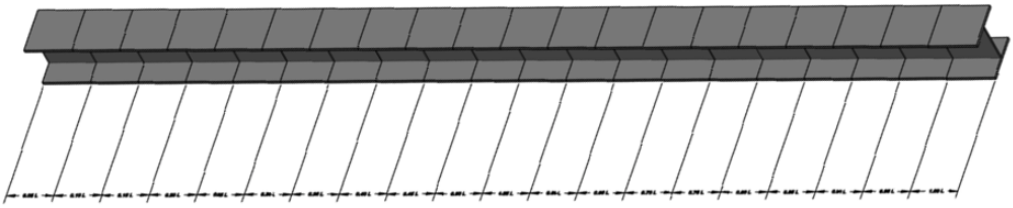

		Length segment ends at																			
Scenario	Worst CS	0.05 L	0.10 L	0.15 L	0.20 L	0.25 L	0.30 L	0.35 L	0.40 L	0.45 L	0.50 L	0.55 L	0.60 L	0.65 L	0.7 L	0.75 L	0.80 L	0.85 L	0.90 L	0.95 L	1.00 L
1	1	1	1	1	1	1	1	1	1	1	1	1	1	1	1	1	1	1	1	1	1
2	2	2	1	1	1	1	1	1	1	1	1	1	1	1	1	1	1	1	1	1	1
3	2	2	2	1	1	1	1	1	1	1	1	1	1	1	1	1	1	1	1	1	1
4	2	2	2	2	1	1	1	1	1	1	1	1	1	1	1	1	1	1	1	1	1
..	...	2	..	2	1	..	..	..	1	..	..	..	..	..	..	..	..	..	..	..	1
..	2	1	1	2	..	..	..	2	1	..	1	..	1	2	..	..	..	..	2	1	1
20	2	2	2	2	2	2	2	2	2	2	2	2	2	2	2	2	2	2	2	2	2
21	3	3	3	3	3	3	3	3	3	3	3	3	3	3	3	3	3	3	3	3	3
22	3	3	2	2	2	2	2	2	2	2	2	2	2	2	2	2	2	2	2	2	2
..	3	3	1	2	2	2	2	2	2	2	2	2	2	2	2	2	2	2	2	2	2
..	3	3	3	1	2	2	2	2	2	2	2	2	2	2	2	2	2	2	2	2	2
..	...	3	3	1	1	2	2	2	2	2	2	2	2	2	2	2	2	2	2	2	2
..	...	3	..	3	..	1	..	..	..	1	2	..	..	..	..	..	..	..	..	..	2
231	3	3	1	1	1	1	1	1	1	1	1	1	1	1	1	1	1	1	1	1	1

Figure 5.11 Example scenarios for condition state distributions along the span

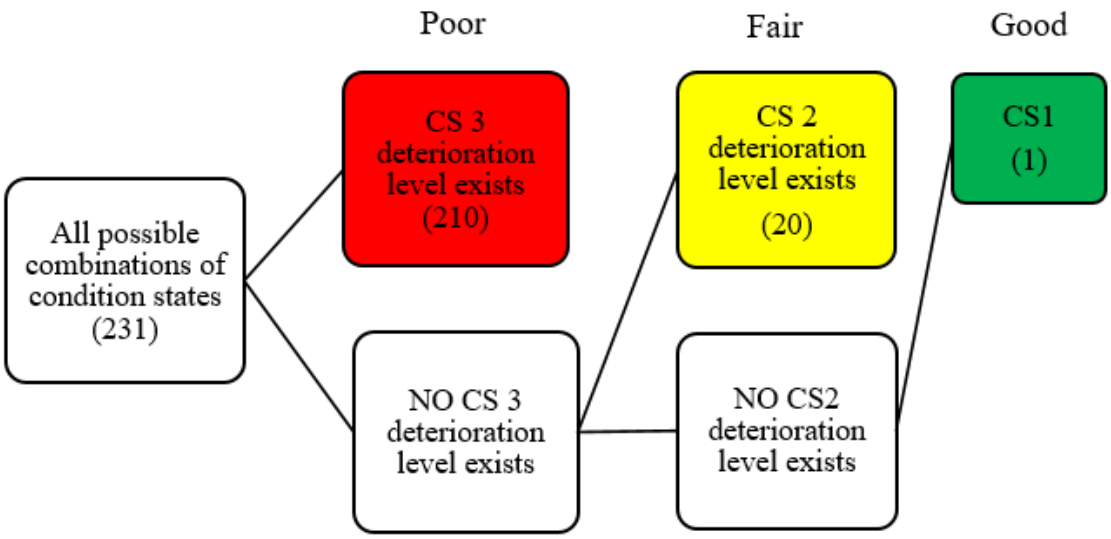

Figure 5.12 Flowchart to categorize CS groups for Approach 1

If the inspection data did not include pictures or any other more detailed information than, for example, 25% CS1, 55% CS2, and 20% CS3, then Approach 2 would be appropriate.

The CS3 blocks could be anywhere along the span (not necessarily all located at the left end, as shown). The possible capacity should reflect that any of CS1, CS2, or CS3 could be present at the critical section near midspan.

The simplest example of this consideration is scenario 2: 5% CS2, 95% CS1. If only the CS proportions are known, then Approach 2 must consider that the CS 2 segment can be anywhere along the span, as shown in Figure 5.13. Approach 3 would be appropriate if inspection data is available to identify which of the particular "Possibilities" in Figure 5.13 is representative of the real bridge. The value for ϕ_c can then be selected as a higher or lower value to reflect the relative uncertainty incorporated in Approaches 2 and 3, respectively.

Scenario	Possibility	CS	All possible distribution of condition state in scenario 2																	
2	1	2	2	1	1	1	1	1	1	1	1	1	1	1	1	1	1	1	1	1
	2	2	1	2	1	1	1	1	1	1	1	1	1	1	1	1	1	1	1	1
	3	2	1	1	2	1	1	1	1	1	1	1	1	1	1	1	1	1	1	1
	4	2	1	1	1	2	1	1	1	1	1	1	1	1	1	1	1	1	1	1
	5	2	1	1	1	1	2	1	1	1	1	1	1	1	1	1	1	1	1	1
	6	2	1	1	1	1	1	2	1	1	1	1	1	1	1	1	1	1	1	1
	7	2	1	1	1	1	1	1	2	1	1	1	1	1	1	1	1	1	1	1
	8	2	1	1	1	1	1	1	1	2	1	1	1	1	1	1	1	1	1	1
	9	2	1	1	1	1	1	1	1	1	2	1	1	1	1	1	1	1	1	1
	10	2	1	1	1	1	1	1	1	1	1	2	1	1	1	1	1	1	1	1
	11	2	1	1	1	1	1	1	1	1	1	1	2	1	1	1	1	1	1	1
	12	2	1	1	1	1	1	1	1	1	1	1	1	2	1	1	1	1	1	1
	13	2	1	1	1	1	1	1	1	1	1	1	1	1	2	1	1	1	1	1
	14	2	1	1	1	1	1	1	1	1	1	1	1	1	1	2	1	1	1	1
	15	2	1	1	1	1	1	1	1	1	1	1	1	1	1	1	2	1	1	1
	16	2	1	1	1	1	1	1	1	1	1	1	1	1	1	1	1	2	1	1
	17	2	1	1	1	1	1	1	1	1	1	1	1	1	1	1	1	1	2	1
	18	2	1	1	1	1	1	1	1	1	1	1	1	1	1	1	1	1	1	2
	19	2	1	1	1	1	1	1	1	1	1	1	1	1	1	1	1	1	2	1
	20	2	1	1	1	1	1	1	1	1	1	1	1	1	1	1	1	1	1	2

Figure 5.13 Possible location of condition state 2 for scenario 2

If the only inspection information available indicates that the worst condition state is CS3 (recalling the previous example with 25% CS1, 55% CS2, 20% CS3), then the bridge could potentially correspond to any one of the 231 scenarios, except the first lines containing only CS1 and CS2. Additionally, each scenario would need to consider all possible realizations for the potential locations of each CS (similar to Approach 2 mentioned above, but also considering other CS proportions, such as 20% CS1/50% CS2/30% CS3, etc.).

Chapter 6: Condition Factor Calculation and Implementation

Selection of condition factors, ϕ_c, should be consistent with the details available from inspections. The four proposed approaches reflect the applicable sources of uncertainty pertinent to each, corresponding to the availability of details from inspections. The approaches described in this chapter incorporate uncertainties identified in the previous chapter, including the representative proportions of each condition state, the locations of condition states along spans, the severity of section loss (% loss) within each condition state, the variation of loss across a section, and the loss due to corrosion in the interim to the next inspection.

Reliability analyses incorporate realizations of potential scenarios (CS at critical section and exact % loss) to quantify expected values (means) and dispersions (standard deviations) for deteriorated flexural capacity at the critical girder section near midspan for a non-deteriorated girder. Individual calculations were performed to assess girder capacity at integer increments of admissible % loss for each CS. The formulation to quantify uncertainty becomes simpler as sources of uncertainty diminish from Approach 1 to Approach 3.

6.1 Approach 1

Approach 1 applies when only the worst condition state in the girders is known. In this approach, simulation of all the possible scenarios (i.e. proportions and locations of condition states) are further categorized into one of the three condition state (CS) groups (refer to Figure 5.12).

6.1.1 Quantifying Uncertainty in Approach 1

In Approach 1, ϕ_c needs to account for the uncertainties due to variation in the amount of corrosion across a section, lack of exact percentage loss within a condition state, unknown location of deterioration and lack of knowledge of the portion of girder in each condition state. The combined uncertainty due to variation in corrosion loss across a section, lack of exact percentage loss in a CS, unknown deterioration location, and unknown proportion of girder total length in each CS, was evaluated using Eq.(25), Eq. (28), and Eq. (31), for CS1, CS2 and CS3 groups, respectively. In Eq. (25) and Eq. (26), the expected capacity (E(CS1)) was calculated using Eq. (23), i.e., by taking the arithmetic average of girder moment capacities, x_i, at each 1% loss increment, *i*, within the CS1 group.

Eq. (26) produces the expected capacity for steel girder bridges with CS2 but without CS3 (E(CS2)). Likewise, Eq. (29) produces the expected capacity with CS3 (E(CS3)). The expected values were calculated using a weighted average of deteriorated moment capacities, weighted proportionately (*a*, *b*, and *c*) to the total girder length associated with condition states 1, 2, and 3. These expected capacities were then used in Eq. (27) and Eq. (30), respectively, to calculate standard deviations within each CS group. The calculated average standard deviation is then increased to account for deterioration variation across a section using an SRSS method (i.e., assuming statistically independent normal variables) as shown in Eq. (28) and (31). The calculations provide representative probabilistic parameters to characterize mean and standard deviation of capacity for each condition state group (CS1, CS2, and CS3) accounting for combined uncertainties in Approach 1.

For CS 1

$$E(CS1) = \frac{\sum_{i=1}^{m} x_i}{m} \tag{23}$$

$$SD(1) = \sqrt{\left(\frac{\sum_{i=1}^{m}\left(\left(x_i - E(CS1)\right)^2\right)}{m-1}\right)} \tag{24}$$

$$SD(CS1) = \sqrt{\left(SD(1)^2 + (E(CS1) * COV_{\max\_1})\text{^}2\right)} \tag{25}$$

Where,

$E(CS1) = Expected\ girder\ moment\ capacity\ in\ the\ CS1\ group$

$SD(CS1) = Standard\ deviation\ of\ girder\ moment\ capacities\ in\ the\ CS\ 1\ group$

$x_i = Girder\ moment\ capacity\ for\ i^{th}\ \%\ loss\ within\ condition\ state\ 1$

$m = \text{N}umber\ of\ \%\ loss\ integer\ increments\ within\ condition\ state\ 1$

$COV_{\max\_1} = COV\ corresponding\ to\ the\ maximum\ \%\ loss\ in\ conditon\ state\ 1$

For CS2

$$E(CS2) = \sum_{s=1}^{20} \frac{\sum_{i=1}^{m} a_s * x_{i,1}/m + \sum_{j=1}^{n} b_s * x_{j,2}/n}{20} \tag{26}$$

$$SD(2) = \sum_{s=1}^{20} \left(\frac{\sqrt{\left(\sum_{i=1}^{m} a_s * \left(x_{i,1} - E(CS2)\right)^2 + \sum_{j=1}^{n} b_s * \left(x_{j,2} - E(CS2)\right)^2 \right) / (m+n-1)}}{20} \right) \tag{27}$$

$$SD(CS\,2) = \sqrt{\left(SD(2)^2 + \left(E(CS2) * COV_{\max\_2}\right)^2\right)} \tag{28}$$

$E(CS2) = Expected\ girder\ moment\ capacity\ in\ the\ CS2\ group$

$SD(CS2) = Standard\ deviation\ of\ plastic\ moment\ capacities\ in\ the\ CS2\ group$

$x_{i,1} = Girder\ moment\ capacitiy\ for\ i^{th}\ \%\ loss\ within\ condition\ state\ 1$

$x_{j,2} = Girder\ moment\ capacitiy\ for\ j^{th}\ \%\ loss\ within\ condition\ state\ 2$

$m = \text{N}umber\ of\ \%\ loss\ integer\ increments\ within\ condition\ state\ 1$

$n = \text{N}umber\ of\ \%\ loss\ integer\ increments\ within\ condition\ state\ 2$

$a_s\ and\ b_s = \%\ length\ of\ girder\ in\ condition\ state\ 1\ and\ 2\ respectively\ for\ s^{th} scenario$

$s = number\ of\ scenarios\ in\ the\ CS2\ group = 20$

$COV_{\max\_2} = COV\ corresponding\ to\ the\ maximum\ \%\ loss\ in\ conditon\ state\ 2$

For CS3

$$E(CS3) = \frac{\sum_{s=1}^{210} \sum_{i=1}^{m} a_s * x_{i,1}/_m + \sum_{j=1}^{n} b_s * x_{j,2}/_n + \sum_{k=1}^{o} c_s * x_{k,3}/_o}{210} \quad (29)$$

$$SD(3) = \sum_{s=1}^{210} \left(\frac{\sqrt{\left(\begin{array}{l} \sum_{i=1}^{m} a_s * \left(x_{i,1} - E(CS3)\right)^2 + \\ \sum_{j=1}^{n} b_s * \left(x_{j,2} - E(CS3)\right)^2 + \\ \sum_{k=1}^{o} c_s * \left(x_{k,3} - E(CS3)\right)^2 \end{array} \right) /_{(m+n+o-1)}}}{210} \right) \quad (30)$$

$$SD(CS\ 3) = \sqrt{\left(SD(3)^2 + \left(E(CS3) * COV_{\max\_3}\right)^2\right)} \quad (31)$$

$E(CS3) = Expected\ girder\ moment\ capacity\ in\ the\ CS3\ group$

$SD(CS3) = Standard\ deviation\ of\ girder\ moment\ capacities\ in\ the\ CS3\ group$

$x_{i,1} = Girder\ moment\ capacitiy\ for\ i^{th}\ \%\ loss\ within\ condition\ state\ 1$

$x_{j,2} = Girder\ moment\ capacitiy\ for\ j^{th}\ \%\ loss\ within\ condition\ state\ 2$

$x_{k,3} = Girder\ moment\ capacitiy\ for\ k^{th}\ \%\ loss\ within\ condition\ state\ 3$

$m = Number\ of\ \%\ loss\ integer\ increments\ within\ condition\ state\ 1$

$n = Number\ of\ \%\ loss\ integer\ increments\ within\ condition\ state\ 2$

$o = Number\ of\ \%\ loss\ integer\ increments\ within\ condition\ state\ 3$

$a_s, b_S\ and\ c_s = \%\ length\ of\ girder\ in\ condition\ state\ 1, 2, and\ 3, respectively, for\ s^{th} scenario$

$s = number\ of\ scenarios\ in\ the\ CS3\ group = 210$

$COV_{\max\_3} = COV\ corresponding\ to\ the\ maximum\ \%\ loss\ in\ conditon\ state\ 3$

6.1.2 Procedure to Find ϕ_c for Approach 1

The values for m, n, and o are the number of % loss increments for which girder capacity was evaluated in condition states 1, 2, and 3 respectively. Girder moment capacities within each condition states are calculated for 1% increments of loss. Values of m, n, and o are summarized in Table 6.1 (see also Table 5.8 and Table 5.11).

Table 6-1 Summary of values of m, n, and o used in Eq. (23) through (31)

		m	n	o
NDOR Distribution Range	**GP 1 & GP 2**	**1**	**1**	**49**
Range Consistent with MBE	**GP 1**	**2**	**6**	**24**
	GP 2	**1**	**5**	**15**

COV_{max} represents the variation in field measurements of deteriorated section thickness variation (refer to 5.1.2 Measurement in the Field) corresponding to the maximum percentage section loss in each scenario. COV_{max} values are shown in Table 6.2.

Table 6-2 Summary of values of COV_{max} used in Eq. (25), (28), and (31)

		COV_{max_1}	COV_{max_2}	COV_{max_3}
NDOR Distribution Range	**GP 1 & GP 2**	**0.01**	**0.01**	**0.045**
Range Consistent with MBE	**GP 1**	**0.01**	**0.038**	**0.045**
	GP 2	**0.01**	**0.028**	**0.045**

Example mean and standard deviation values obtained for the capacity of a W30x99 girder with GP1 and GP2 deterioration profiles are provided in Table 6.3.

Table 6-3 Sample mean and standard deviation for CS's with GP1 and GP2

	GP 1		GP 2	
W30X99	**Mean**	**Std. Dev.**	**Mean**	**Std. Dev.**
CS 1	**1806**	**18.1**	**1776**	**17.8**
CS 2	**1801**	**68.5**	**1767**	**67.4**
CS 3	**1710**	**150.5**	**1613**	**225**

A range of span lengths and girder spacings were considered in the reliability analyses. Span lengths ranged from 50 ft to 120 ft with an increment of 10 ft. Girder spacings varied from 3.5 to 7 ft with an increment of 0.5 ft. The change in length and girder spacing directly affects the Girder Distribution Factor (GDF), which was determined according to AASHTO LRFD Specifications. These variations resulted in a total of (8 * 8 =) 64 cases. A total of 64 structural configurations * 3 CS classifications = 192 reliability analyses were performed to obtain ϕ_c values consistent with a target reliability index of 3.5. Possible future corrosion was reflected through a bias factor, as discussed in the previous chapter.

6.1.3 ϕ_c for Approach 1

Baseline ϕ_c values applicable to each CS group for Approach 1 are provided in Table 6.4 for carbon steel in a rural environment, obtained by averaging the 64 values obtained for each CS with various structural configurations. As discussed in the previous chapter, multipliers to be applied to ϕ_c are provided in Table 6.5 for evaluations of bridges in more corrosive environments than NCHRP 301 “rural” conditions. Similarly, multipliers are provided in Table 6.6 for weathering steel in any environment. The multipliers are also averages to represent the considered structural configurations (span and girder spacing). Calibrated values for both baseline ϕ_c values and multipliers are provided for separate analyses of GPs and CS % loss ranges.

Table 6-4 ϕ_c for carbon steel when the worst CS is known in a rural environment

Carbon Steel in Rural Environment		CS 1	CS 2	CS 3
NDOR Distribution Range	GP 1	0.99	0.94	0.69
	GP 2	0.98	0.94	0.42
Range Consistent with MBE	GP 1	0.99	0.93	0.80
	GP 2	0.98	0.92	0.75

Table 6-5 Multiplier for ϕ_c for carbon steel in urban and marine environment

		Carbon Steel					
		Urban Environment			Marine Environment		
Multiplier for		ϕ_c 1	ϕ_c 2	ϕ_c 3	ϕ_c 1	ϕ_c 2	ϕ_c 3
NDOR Distribution Range	GP 1	0.98	0.98	0.97	0.97	0.97	0.96
	GP2	0.96	0.96	0.93	0.95	0.95	0.91
Range Consistent with MBE	GP 1	0.98	0.98	0.97	0.97	0.97	0.96
	GP2	0.96	0.96	0.95	0.95	0.95	0.94

Table 6-6 Multiplier for ϕ_c for weathering steel in the three environments

		Weathering Steel								
		Rural Environment			Urban Environment			Marine Environment		
Multiplier for		ϕ_c 1	ϕ_c 2	ϕ_c 3	ϕ_c 1	ϕ_c 2	ϕ_c 3	ϕ_c 1	ϕ_c 2	ϕ_c 3
NDOR Range	GP 1	1.00	1.00	1.00	0.99	0.99	0.99	0.99	0.99	0.99
	GP2	1.00	1.00	1.00	0.98	0.98	0.96	0.98	0.98	0.97
Consistent with MBE	GP 1	1.00	1.00	1.00	0.99	0.99	0.99	0.99	0.99	0.99
	GP2	1.00	1.00	1.00	0.98	0.98	0.98	0.98	0.98	0.98

The MBE indicates that load ratings should be performed using only sound material area, but Approach 1 only applies when no information is available to enable such rigor. Instead, the authors propose that a % loss is implemented on the deteriorated regions of girders according to

GP1 or GP2, as appropriate, according to Table 6.7. These section property penalties will produce results similar to the reliability analyses performed in this research to generate ϕ_c.

Table 6-7 Percentage loss for condition states in Approach 1

Distribution Profile	Condition State	Percentage Loss to use for Load Rating
GP 1	1	0.5%
	2	2.3%
	3	8.4%%
GP 2	1	0%
	2	1.3%
	3	7.2%
NDOR's Range (Both Profiles)	1	0 %
	2	0.26%
	3	9.5%

6.2 Approach 2

Approach 2 is applicable when the relative CS proportions present along the girders are known, but not the locations along spans where particular condition states are located. For example, all deterioration distributions along the span in Figure 6.1 would be evaluated identically according to Approach 2. In most cases shown, the critical flexural section is CS1, but in some instances CS2 or CS3 could occur at or near the critical section (for instance, if the deck had cracked near midspan, allowing de-icing chemicals to penetrate through the concrete from the road surface to the steel). The total CS3 and CS2 proportions along the length would be known, but the load rating engineer could not differentiate between the possible distributions shown unless more information was available (in which case, Approach 3 would be appropriate).

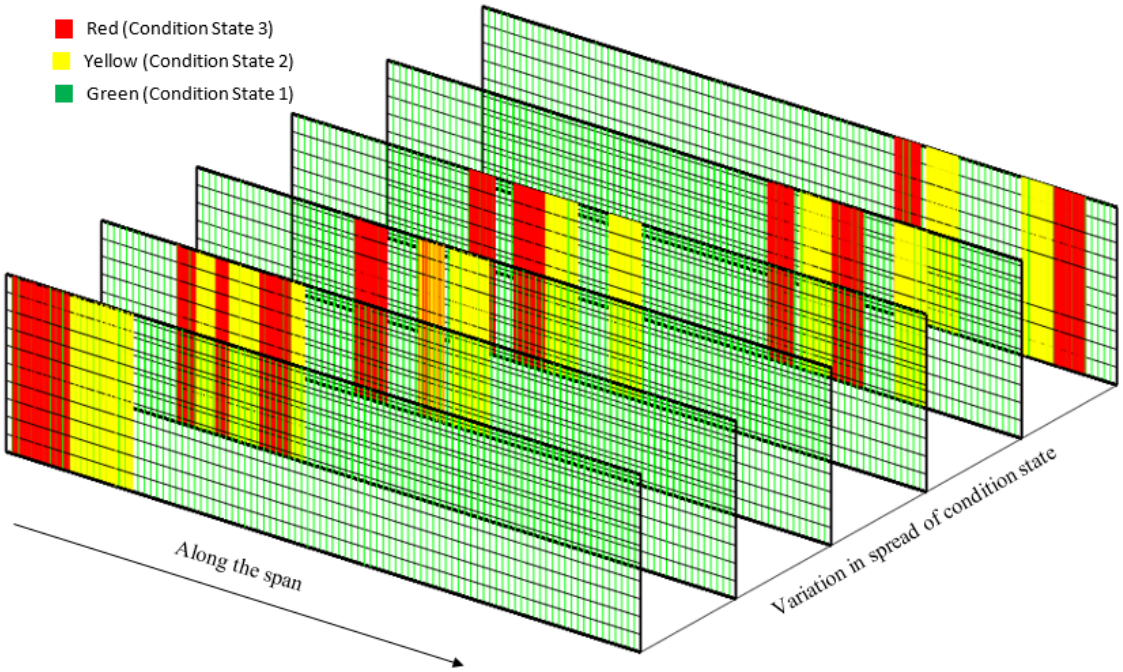

Figure 6.1 Sample of possible distribution for one of the scenarios

6.2.1 Quantifying Uncertainty in Approach 2

In Approach 2, ϕ_c needs to account for the uncertainties due to variation in the amount of corrosion across a section, lack of exact percentage loss in a CS, and unknown location of deterioration. The procedure to address these uncertainties is similar to that presented in Section 6.1.1 Quantifying Uncertainty in Approach 1. The combined uncertainty due to variation in the amount of corrosion across a section, lack of exact percentage loss in a CS, and unknown location of deterioration was evaluated using Eq. (34). The expected capacity for each scenario (where a "scenario" refers to a particular proportionate distribution of condition states) was calculated using the weighted average of girder moment capacities proportionate to the presence of each CS, as indicated in Eq. (32). The expected capacity is used in Eq. (33) to calculate the standard deviation from weighted variances using CS proportions as weights. Finally, the girder capacity standard deviation is calculated by using the SRSS of the value in Eq. (33) and the

standard deviation from the variation across a section associated with the maximum percentage loss (see section 5.1 Uncertainties in Section Deterioration).

$$E(capacity) = \sum_{j=1}^{3} p_j * \mu_{cs_j} \tag{32}$$

$$SD = \sqrt{\frac{\sum_{j=1}^{3}\sum_{i=1}^{m_j} p_j \left(x_{i,j} - E(capacity)\right)^2}{\left(\sum_{j=1}^{3} m_j\right) - 1}} \tag{33}$$

$$SD(capacity) = \sqrt{SD^2 + \left(E(Capacity) * COV_{\max\_j}\right)^2} \tag{34}$$

Where,

$E(capacity) = Expected\ girder\ moment\ capacity\ for\ a\ scenario$

$SD(capacity) = Standard\ deviation\ of\ girder\ moment\ capacities\ in\ a\ scenario$

$j = 1, 2, or\ 3\ for\ CS1, CS2, or\ CS3, respectively$

$p_j = percentage\ of\ girder\ in\ j^{th} condition\ state$

$m_j =$ n$umber\ of\ \%\ loss\ integer\ increments\ within\ j^{th}\ condition\ state$

$\mu_{cs_j} = expected\ girder\ moment\ capacity\ within\ j^{th}\ condition\ state$

$x_{i,j} = girder\ moment\ capacity\ with\ i^{th}\ \%\ loss\ within\ j^{th}\ condition\ state$

$COV_{\max\_j} = COV\ associated\ with\ the\ max\ \%\ loss\ in\ j^{th} condition\ state$

Eq. (32), Eq. (33), and Eq. (34) are effectively identical to Eq. (29), Eq. (30), and Eq. (31) (from Approach 1 with CS3) executed for only a single value of the "s" scenario counter.

The p_j term in Eq. (32) and Eq. (33) corresponds to a_s, b_s, and c_s in Eq. (29) and Eq. (30). Similarly, the m_j takes the place of m, n, and o. $COV_{\max\_j}$ represents COV_{max_1}, COV_{max_2}, and COV_{max_3} in Approach 1 (see Table 6.2).

Structural configurations with various combinations of span lengths and girder spacings were considered for Approach 2 similarly to Approach 1. For Approach 2, however, the 64 potential combinations needed to be evaluated for each of the 231 possible CS combination scenarios, rather than only for the 3 general CS groups. The relationship between ϕ_c and expected moment capacity is nonlinear, as shown in Figure 6.2.

Each point represents a combination of ϕ_c and deteriorated moment capacity for a particular combination of condition states. As CS3 increases, the moment capacity decreases (trending to the left in the figure). Similarly, maximum capacity (farthest right) corresponds a girder entirely in CS1. In the middle region, various combinations of condition states can possess similar mean capacity, yet have wider dispersion of possible simulated capacity (CS1 vs CS3 at the critical section). For example, two bridges may have unique and distinct proportionate combinations of CS1, CS2, and CS3, and simultaneously have similar expected capacities. One bridge may have proportionately more CS2 than CS3, and the other bridge may have more CS3 than CS2 (and also more CS1, maintaining a similar expected capacity on average). The bridge with more CS1 and CS3 would have greater variation in the potential capacity at the critical section, and this greater uncertainty would correspond to a lower ϕ_c.

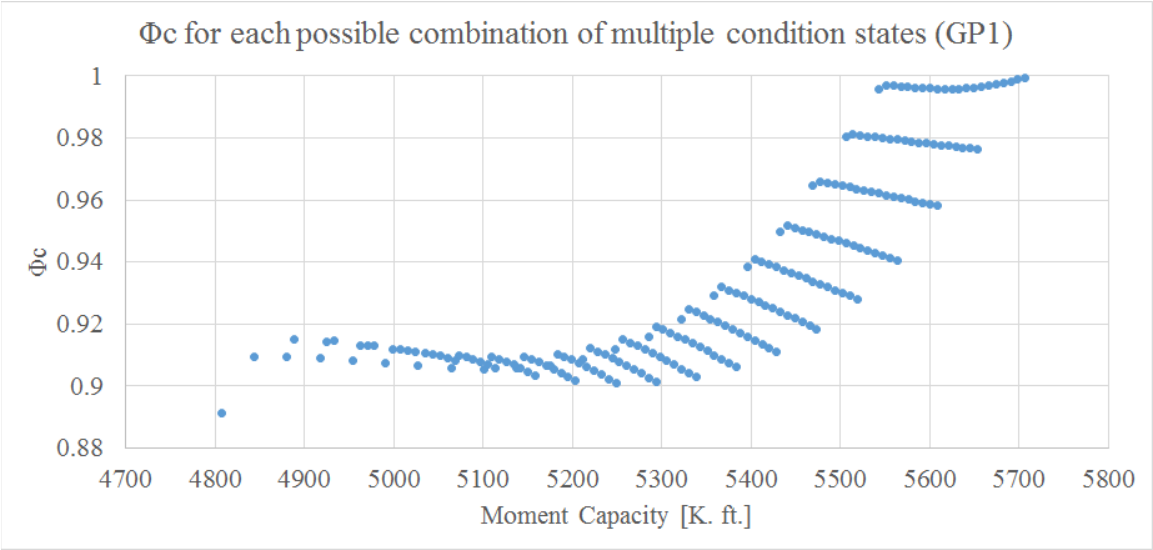

Figure 6.2 Moment capacity VS ϕ_c for the 231 combinations

6.2.2 Artificial Neural Networks (ANNs)

Artificial Neural Networks (ANNs) are a biologically inspired computer program designed to simulate the way the human brain processes the information to detect patterns and relationships in data and learn through experience (Agatonovic-Kustrin & Beresford, 2000). ANNs are trained to predict outcomes from a suite of known input-output scenarios until the output error predictions are minimized and the network reaches a specified level of accuracy.

ANNs were used in this study as a nonlinear, multivariate prediction tool to estimate ϕ_c values for Approach 2. An ANN was trained using the percentage in each condition state as the input and analytically obtained ϕ_c values as the output. Over 14700 inputs were supplied to the neural network toolbox in MATLAB for ANN training, validation, and testing. The particular ANN architecture implemented for this study used 10 neurons in a single hidden layer to predict

ϕ_c for Approach 2 from the 3 proportionate percentages present for each CS in a particular scenario, as shown in Figure 6.3.

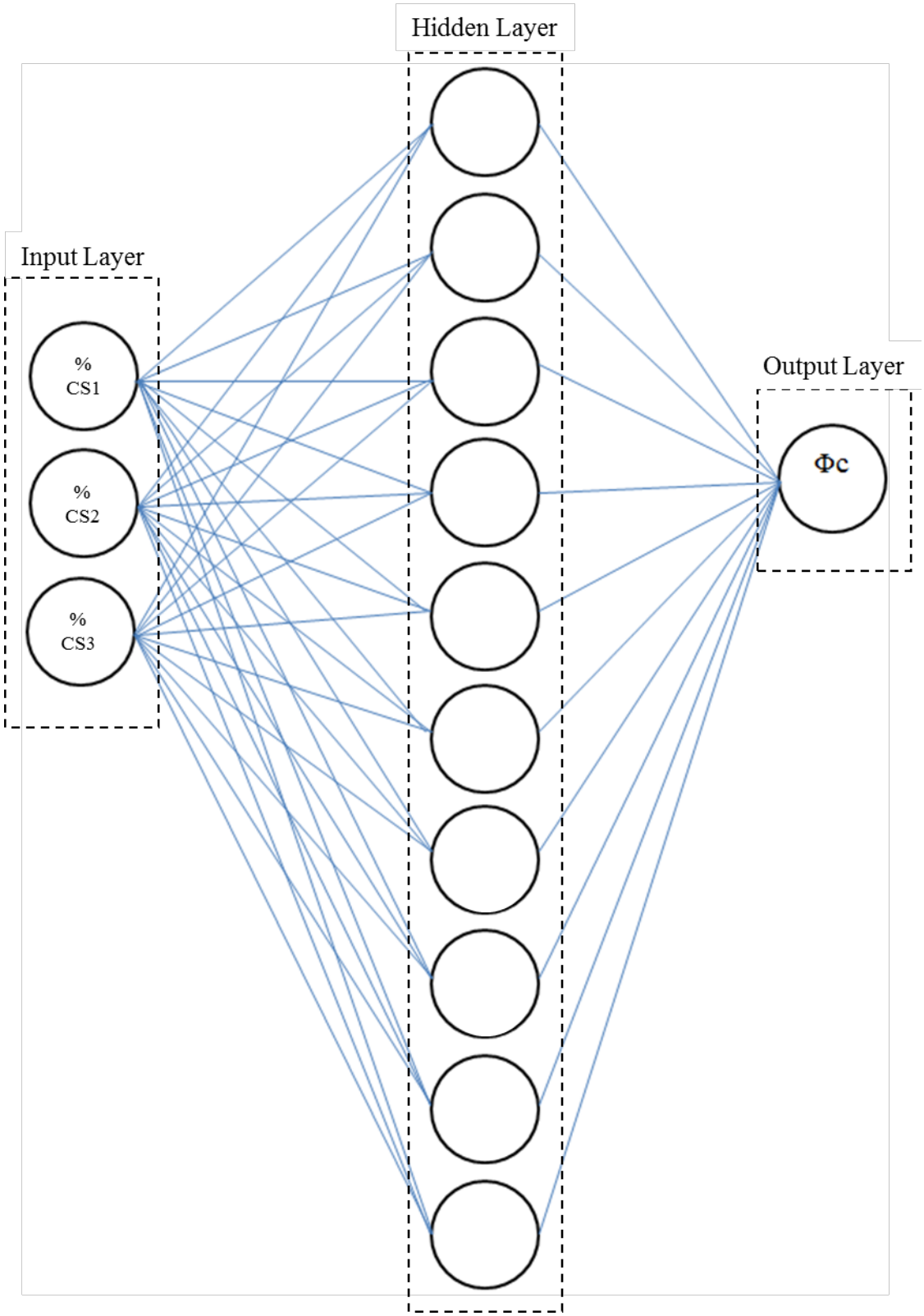

Figure 6.3 Neural network architecture

The default mathematical framework available from the Neural Network Toolbox was implemented for this study, with a log-sigmoid transfer function in the hidden layer, and a linear summation at the output layer. To manually evaluate the ANN, after weight and bias values have been obtained from training, the first step is to calculate inputs, n_i, to each of the *i* hidden transfer functions:

$$n_i = \left[w_{hidden\_i,input\_CS}\right]_{1x3} \begin{Bmatrix} \%\ CS1 \\ \%\ CS2 \\ \%\ CS3 \end{Bmatrix}_{3x1} + b_i \tag{35}$$

With 10 hidden neurons, the *i* subscript ranges from 1 to 10. 3 weights, *w*, are associated with each neuron. One scalar weight value corresponds to each % condition state. A bias term, b_i, is added to the result of weights multiplied by % CS inputs, for each neuron, *i*. The resulting *n* values are passed through a log-sigmoid transfer function ranging from -1 to 1, which will become inputs, *a*, to the output layer from each of the *i* hidden neurons:

$$a_i = \frac{2}{1 + e^{-2n_i}} - 1 \tag{36}$$

The final step is to apply output layer weights, w_{output}, to the values exiting the hidden layer, *a*, sum the 10 results (shown in the equation below as a vector multiplication), and add a final bias term to obtain a single scalar result, ϕ_c:

$$\phi_c = \left[w_{output}\right]_{10x1}{}^{T} [a]_{10x1} + b_{output} \tag{37}$$

6.2.3 ϕ_c for Approach 2

To account for sound material area, an expected capacity can be determined which will be approximately consistent with the mean value obtained during and implemented in the reliability analyses. The expected capacity can be determined using a representative % loss obtained from Eq. (38), supplemented with the values provided in Table 6.8.

$$\%\ loss = Portion_{cs} * \%\ Loss_{CS1} + Portion_{cs2} * \%\ Loss_{CS2} + Portion_{cs3} * \%\ Loss_{CS3} \quad (38)$$

Table 6-8 Representative percentage loss for each condition state with Approach 2

Distribution Profile	Condition State	Percentage Loss for Load Rating
GP 1	1	0.5%
	2	4%
	3	19%
GP 2	1	0
	2	2.5%
	3	12.5%
NDOR's Range (Both Profiles	1	0 %
	2	0.5%
	3	25.5%

Values obtained from ANN training, to be used in Eq. (35) and Eq. (37), are provided in Table 6.9 through Table 6.12. Weight and bias values have been calibrated for each deterioration profile, GP, and for both MBE-consistent and current NDOR section loss ranges.

Table 6-9 ANN coefficients for GP1 deterioration profile

GP1 with range consistent with MBE						
	Hidden Layer				Output Layer	
	CS_1 %	CS_2 %	CS_3%	Bias	Weights	Bias
W_1	1.93	-1.92	0.82	-3.06	0.19	-0.12
W_2	1.79	1.61	-1.17	-2.97	0.05	
W_3	-1.59	1.90	1.49	1.77	-0.05	
W_4	2.01	-0.01	2.42	-1.23	-0.83	
W_5	0.60	1.92	2.47	-0.38	-0.83	
W_6	-2.09	-1.92	0.51	0.63	-0.95	
W_7	-1.12	-1.33	2.07	-1.13	0.17	
W_8	0.38	2.86	-0.61	1.52	0.01	
W_9	1.82	2.03	1.48	1.85	1.54	
W_10	1.54	1.75	-0.81	2.99	-0.59	

Table 6-10 ANN coefficients for GP2 deterioration profile

GP2 with range consistent with MBE						
	Hidden Layer				Output Layer	
	CS_1 %	CS_2 %	CS_3%	Bias	Weights	Bias
W_1	-0.98	-1.40	0.46	0.87	3.28	0.437
W_2	-2.10	3.35	-1.94	3.78	3.23	
W_3	-0.58	-0.35	-2.17	-2.41	4.22	
W_4	4.62	-2.94	3.30	-5.35	3.15	
W_5	1.07	-2.23	-2.24	1.00	-1.05	
W_6	4.26	-0.80	1.66	-1.65	0.04	
W_7	2.30	-1.46	-1.44	1.83	0.37	
W_8	-3.99	2.29	-3.88	2.16	-1.39	
W_9	-2.56	0.27	0.33	-3.31	-1.84	
W_10	1.15	-1.05	3.84	-3.93	-0.30	

Table 6-11 ANN coefficients for GP 1 deterioration profile with NDOR Range

GP1 with range consistent with current NDOR policy						
	Hidden Layer				Output Layer	
	CS_1 %	CS_2 %	CS_3%	Bias	Weights	Bias
W_1	1.04	1.09	-1.67	-3.8819	-0.13	0.024
W_2	1.04	0.99	-2.09	-2.4450	1.03	
W_3	-0.40	2.84	0.01	1.8869	0.30	
W_4	1.85	-1.82	1.35	-0.6974	0.21	
W_5	1.05	0.96	-0.95	-0.2376	0.46	
W_6	2.35	-2.01	0.25	0.3942	-0.02	
W_7	-0.42	-2.34	0.20	-1.4051	0.09	
W_8	-2.92	1.12	0.74	-1.8546	0.02	
W_9	0.85	0.02	-1.03	2.5113	1.03	
W_10	0.87	1.71	-1.78	3.4655	-0.08	

Table 6-12 ANN coefficients for GP2 deterioration profile with NDOR Range

GP2 with range consistent with current NDOR policy						
	Hidden Layer				Output Layer	
	CS_1 %	CS_2 %	CS_3%	Bias	Weights	Bias
W_1	-0.18	1.21	2.13	3.19	-0.02	0.261
W_2	0.68	-1.17	-2.38	-2.11	0.03	
W_3	2.02	-2.23	2.31	-3.64	-0.24	
W_4	0.93	1.27	2.78	-1.32	-0.71	
W_5	1.90	1.91	1.51	-0.64	-0.59	
W_6	0.47	2.59	2.61	-0.42	-1.07	
W_7	-1.97	1.15	1.25	-2.04	0.25	
W_8	-2.28	-2.30	-0.77	-0.99	-0.66	
W_9	-1.66	-1.75	-1.65	-2.49	-1.12	
W_10	-0.13	-0.20	-3.18	-4.33	3.12	

The ANNs provided reliable estimations to correlate CS proportions to values of ϕ_c for bridge evaluation. Each set of ANN fitting parameters is described below, with a figure showing the general trend of ANN-predicted values on vertical axes versus on rigorous condition factors obtained by full reliability analyses the horizontal axes. Ideally, the results would follow a perfect linear trend line of $y = 1.00x$, with an R^2 of 1. The frequencies of relative error magnitudes are not evident when only plotting analytical versus predicted values, so histograms are also provided to accompany each trend line plot. The standard error is also specified for each case. Ninety-five percent and 99% lower bound offsets approximately correspond to 2 and 3 standard errors, respectively.

Trend lines are shown for ANN predictions versus analytically determined ϕ_c values, together with accompanying histograms of ANN prediction errors in Figure 6.4 and Figure 6.5 for MBE-consistent % loss ranges in each CS and GP1, in Figure 6.6 and Figure 6.7 for MBE-consistent % loss ranges in each CS and GP2, in Figure 6.8 and Figure 6.9 for NDOR-consistent % loss ranges in each CS and GP1, and in Figure 6.10 and Figure 6.11 for NDOR-consistent % loss ranges in each CS and GP2.

Standard errors were 1.03×10^{-4} and 4.24×10^{-5}, and the most unconservative prediction errors were 0.036 and 0.012 for MBE-consistent % loss ranges with GP1 and GP2, respectively. Standard errors were 1.77×10^{-4} and 9.48×10^{-5}, and the most unconservative prediction errors were 0.062 and 0.041 for NDOR-consistent % loss ranges with GP1 and GP2, respectively.

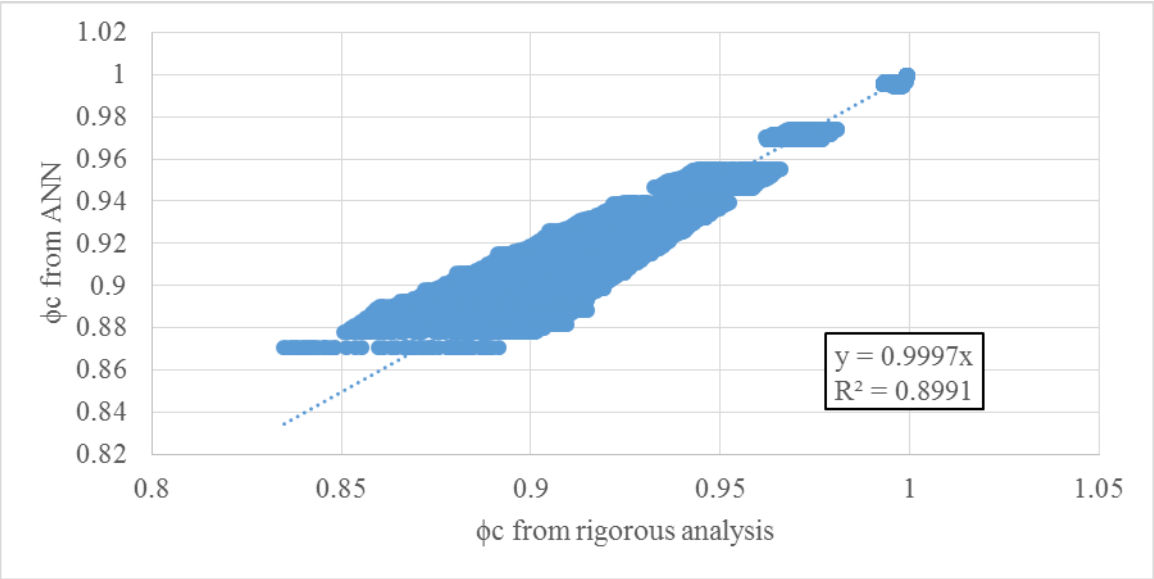

Figure 6.4 ANN ϕ_c prediction errors for MBE-consistent deterioration ranges and GP1

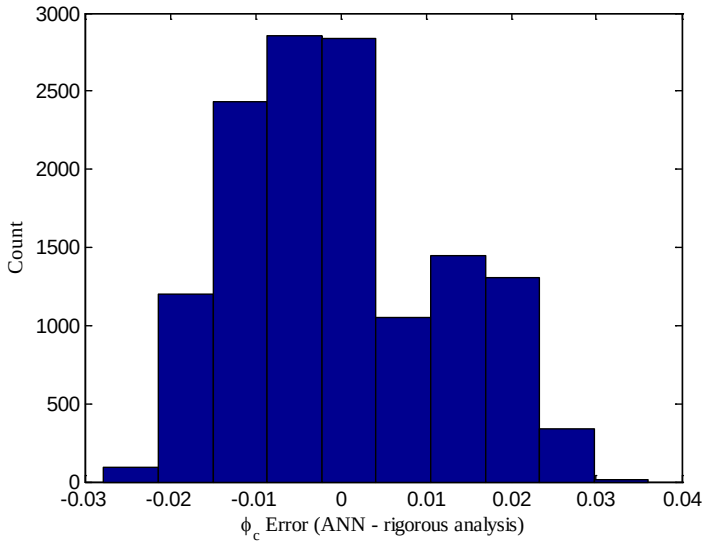

Figure 6.5 Histogram of ANN ϕ_c prediction errors: MBE & GP1

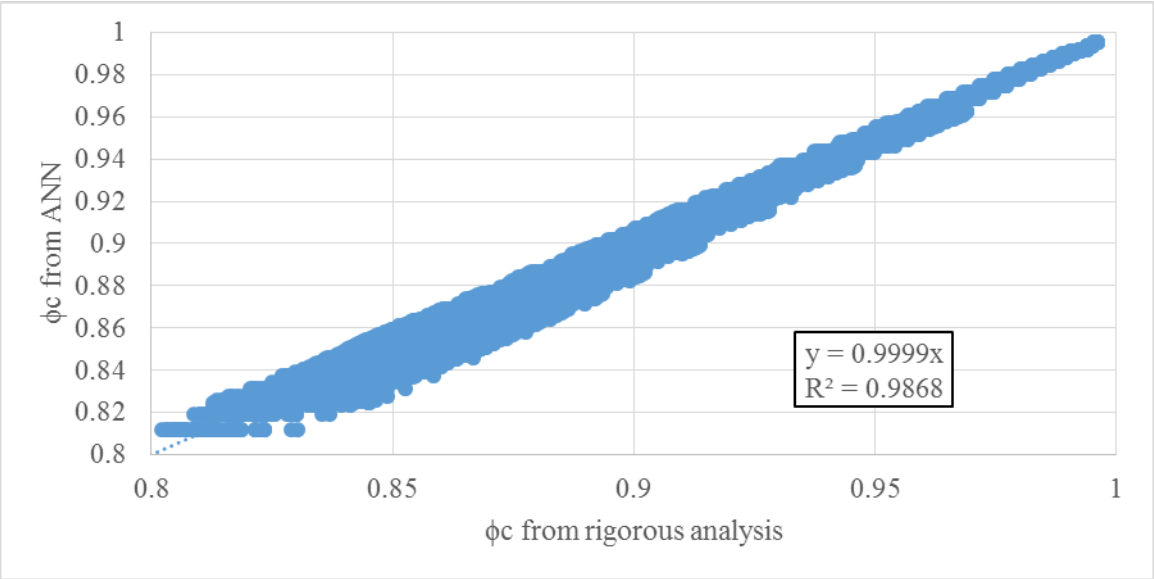

Figure 6.6 ANN ϕ_c prediction errors for MBE-consistent deterioration ranges and GP2

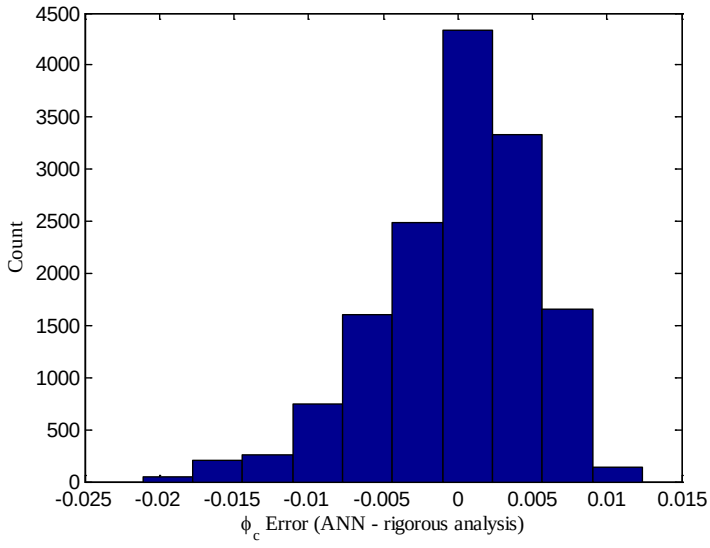

Figure 6.7 Histogram of ANN ϕ_c prediction errors: MBE & GP2

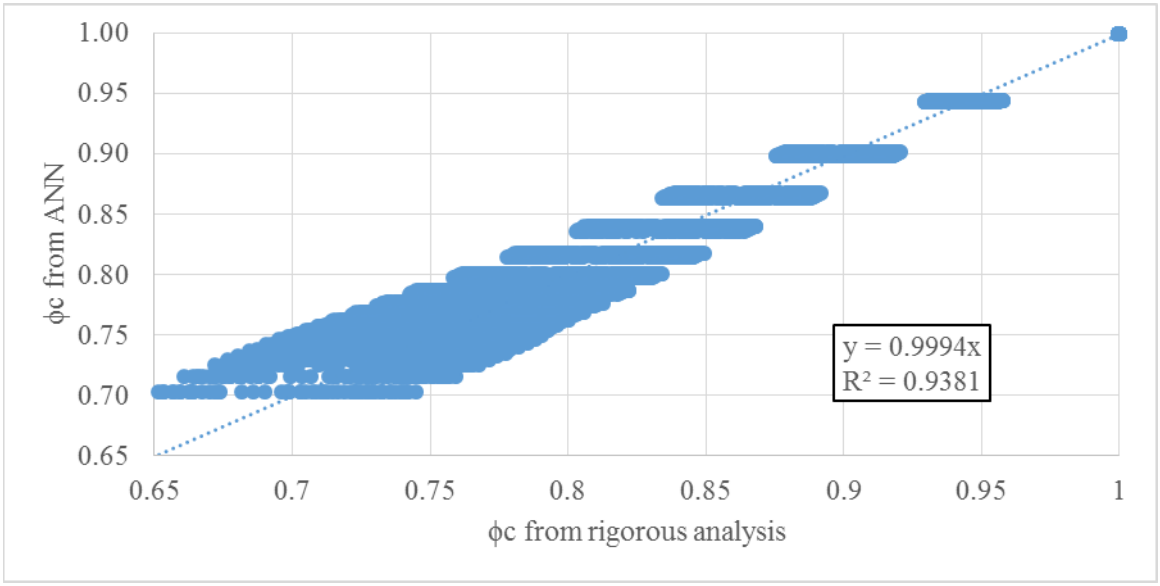

Figure 6.8 ANN ϕ_c prediction errors for NDOR-consistent deterioration ranges and GP1

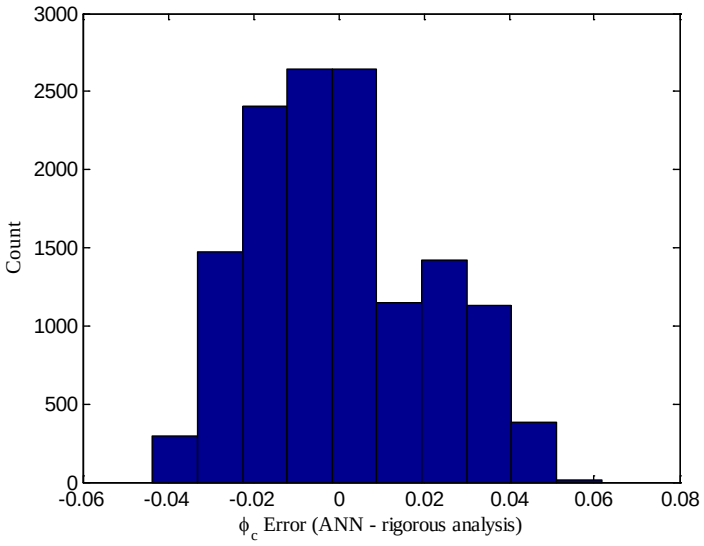

Figure 6.9 Histogram of ANN ϕ_c prediction errors: NDOR & GP1

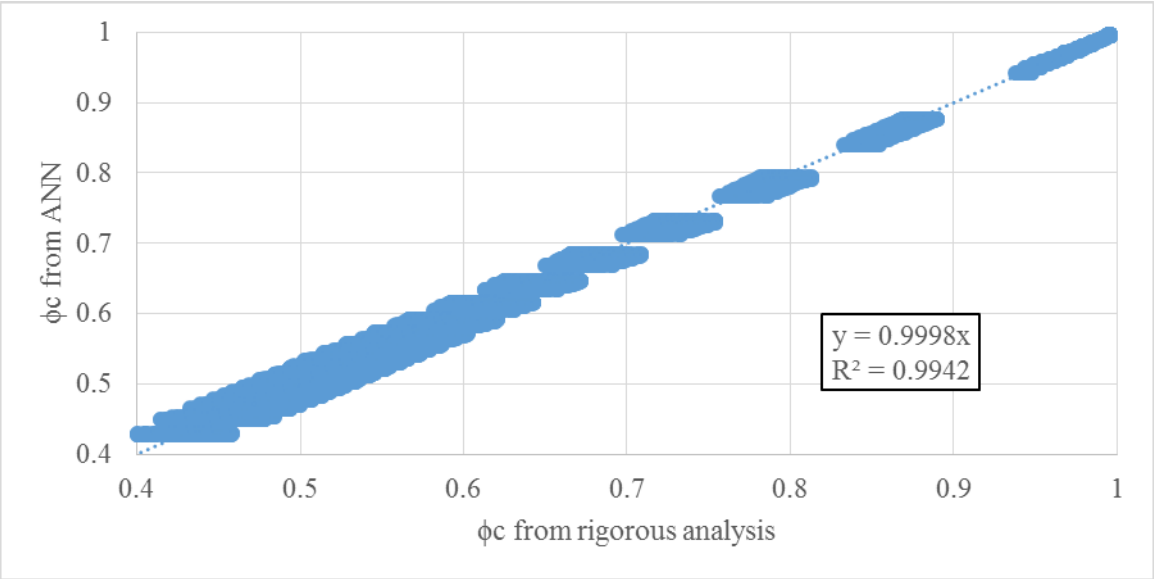

Figure 6.10 ANN ϕ_c prediction errors for NDOR-consistent deterioration ranges and GP2

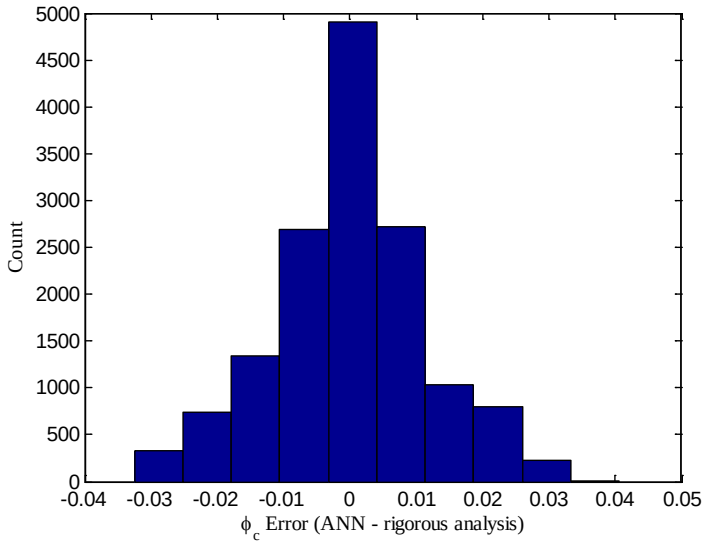

Figure 6.11 Histogram of ANN ϕ_c prediction errors: NDOR & GP2

6.3 Approach 3

Approach 3 applies when the locations of deteriorated sections are known along girder span, in addition to knowing the proportion of length over which particular condition states have occurred. In this approach, engineers need to model an equivalent condition state % loss at the locations noted in the field. An example of the distribution of condition states in a girder is shown in Figure 6.12. This hypothetical girder with a length of 50 ft. has condition state 2 in the first 5 ft (10% of total length), then progressing along the length, 13 ft (26%) in condition state 1, 10 ft (20%) in condition state 3, 17 ft (34%) in condition state 1, and 5 ft (10%) in condition state 2. If this distribution along the span was not known, the girder could be evaluated using Approach 2, knowing that 60% of the girder is in CS1, 20% of the girder is in CS2, and 20% of the girder is in CS3. Or, if the proportions of condition states are known, the bridge could be evaluated using the general CS3 category in Approach 1.

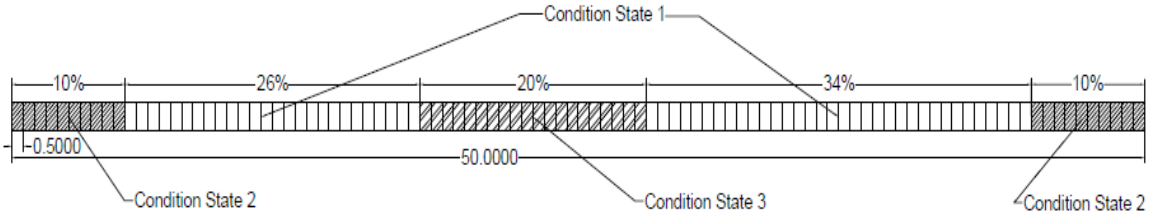

Figure 6.12 Example condition state distribution along girder length

Knowing the distribution of condition states along the span, it should be feasible to perform a load rating analysis accounting for the variation in induced load effects in addition to uncertain capacity at any particular condition state. The previous methods presumed that the

critical section occurred at the non-deteriorated girder critical section, but the true critical section can be identified when deterioration locations are known along the span.

6.3.1 Quantifying Uncertainty in Approach 3

In Approach 3, the ϕ_c must account for the uncertainties due to variation in the amount of corrosion across a section and unknown (exact) percentage loss within a condition state. These uncertainties are addressed similarly to previously described methods in Section 6.1.1 Quantifying Uncertainty in Approach 1. Consequently, the combined uncertainty due to variation in the amount of corrosion, and unknown exact percentage loss can be evaluated using Eq. (41) for any of the three condition states. In Eq. (40) and Eq. (41), the expected capacity (E (CSj)) is calculated using Eq. (39), i.e. by taking arithmetic average of girder moment capacities, $x_{i,j}$, at each 1% loss increment, *i*, within each CS group, *j*. The variation due to lack of exact percentage loss is calculated using Eq. (40), which is combined using SRSS to the standard deviation accounting for uncertain % loss variation across a section, as shown in Eq. (41).

$$E(CSj) = \frac{\sum_{i=1}^{n} x_{i,j}}{m_j} \tag{39}$$

$$SD = \sqrt{\left(\frac{\sum_{i=1}^{m_j}\left(\left(x_{i,j} - E(CSj)\right)^2\right)}{m_j - 1}\right)} \tag{40}$$

$$SD(CSj) = \sqrt{\left(SD^2 + (E(CSj) * COV_{\max\_j})\text{^}2\right)} \tag{41}$$

Where,

$j = 1, 2\ or\ 3\ for\ conditon\ state\ 1, 2\ or\ 3\ respectively$

$x_{i,j} = \ percentage\ of\ girder\ with\ i^{th}\ \%\ loss\ in\ j^{th} condition\ state$

$E(C\ S\ j) =$ *Expected plastic moment capacity of condition state j*

$SD(C\ S\ j) =$ *Standard deviation of the* j^{th} *condition state*

$m_j =$ *number of plastic moment capacity in* j^{th} *condition state.*

$COV_{\max\_j} =$ *COV associated with the max percentage loss in* j^{th} *condition state*

6.3.2 ϕ_c for Approach 3

For Approach 3, it is appropriate to apply individual ϕ_c values for each CS region. For bridges with carbon steel and subject to minor future deterioration ("rural" environments, per NCHRP 301), ϕ_c values for each CS can be selected from Table 6.13, as appropriate to the ranges of deterioration guiding assignment of condition states during the inspection, and the prevalent deterioration profile (GP1 with bottom flange and web only, GP2 for full depth deterioration). If the bridge was constructed with weathering steel and/or subject to more severe future deterioration than "rural" conditions, the values obtained from Table 6.14 or Table 6.15.

Table 6-13 ϕ_c for each condition state and the range of percentage loss

	Condition State 1 range	Condition State 2 range	Condition State 3 range	ϕ_c for Condition State 1	ϕ_c for Condition State 2	ϕ_c for Condition State 3
NDOR Range with GP1 deterioration	0%	0-1%	1-50%	1.00	1.00	0.70
NDOR Range with GP2 deterioration	0%	0-1%	1-50%	1.00	1.00	0.40
MBE GP 1	0-1%	1-7%	7-35%	1.00	0.95	0.87
MBE GP 2	0%	0-10%	10-30%	1.00	0.94	0.85

Table 6-14 Multipliers to ϕ_c for carbon steel in urban and marine environment

		Carbon Steel					
		Urban Environment			Marine Environment		
Multiplier for		ϕ_c 1	ϕ_c 2	ϕ_c 3	ϕ_c 1	ϕ_c 2	ϕ_c 3
NDOR Distribution Range	GP 1	0.98	0.98	0.97	0.97	0.97	0.96
	GP2	0.96	0.96	0.93	0.95	0.95	0.91
Range Consistent with MBE	GP 1	0.98	0.98	0.97	0.97	0.97	0.96
	GP2	0.96	0.96	0.95	0.95	0.95	0.94

Table 6-15 Multipliers to ϕ_c for weathering steel in the three environments

		Weathering Steel								
		Rural Environment			Urban Environment			Marine Environment		
Multiplier for		ϕ_c 1	ϕ_c 2	ϕ_c 3	ϕ_c 1	ϕ_c 2	ϕ_c 3	ϕ_c 1	ϕ_c 2	ϕ_c 3
NDOR Range	GP 1	1.00	1.00	1.00	0.99	0.99	0.99	0.99	0.99	0.99
	GP2	1.00	1.00	1.00	0.98	0.98	0.96	0.98	0.98	0.97
Consistent with MBE	GP 1	1.00	1.00	1.00	0.99	0.99	0.99	0.99	0.99	0.99
	GP2	1.00	1.00	1.00	0.98	0.98	0.98	0.98	0.98	0.98

Similar to Approaches 1 and 2, an approximate adjustment to section properties is proposed to account for sound material and correspond to the reliability analyses performed to produce the ϕ_c factors. As in Approach 1, tabulated values are provided in Table 6.16 to produce appropriate reduced sound material section properties.

Table 6-16 Percentage loss for each condition state in Approach 3

Distribution Profile	Condition State	Percentage Loss to use for Load Rating
GP 1	**1**	0.5%
	2	4%
	3	19%
GP 2	**1**	0%
	2	2.5%
	3	12.5%
NDOR's Range (Both Profiles	**1**	0 %
	2	0.5%
	3	25.5%

6.4 Special Approach

The concept of ϕ_c was introduced in NCHRP 301 to account for future corrosion and increased variability in section properties for the deteriorated member. Standard procedures do not explicitly require measurement of remaining section, only requiring that load ratings should be based on "sound material" remaining. If a section loss is noted, the value is typically a visual estimate rather than a true measurement. The lack of measurements from the field and the concept of condition state as a range of section loss combine together to introduce a substantial source of uncertainty in load ratings. If field measurements are available, the uncertainty associated with the sound material remaining would be greatly reduced.

If a special inspection is performed, and measurement values and locations are noted in inspection documentation, the only remaining uncertainties to address with ϕ_c would be increased variability across the section (see 5.1 Uncertainties in Section Deterioration) and future section loss between inspections (see 5.2 Future Corrosion). Reliability analyses were performed for all percentage loss increments from 0 to 50%, accounting for the COV for section variability and the bias for future corrosion. Percent loss thresholds are noted in Table 6.17, corresponding

to 0.05 increments of ϕ_c for carbon steel in rural environments. Other steel and/or environment conditions should be adjusted by the modifiers in the appropriate column, multiplied by the basic value for carbon steel in rural environments.

Table 6-17 ϕ_c and multiplier for different range of deterioration

	Carbon Steel			Weathering Steel		
Percentage loss	**Rural**	**Urban**	**Marine**	**Rural**	**Urban**	**Marine**
Up to 3.0%	1.00	*1.00	*1.00	*1.00	*1.00	*1.00
Up to 8.0%	0.95	*1.00	*1.00	*1.00	*1.00	*1.00
Up to 28.0%	0.90	*0.95	*0.95	*1.00	*1.00	*1.00
Up to 45.0%	0.85	*0.95	*0.95	*1.00	*1.00	*1.00
Up to 50.0%	0.80	*0.95	*0.95	*1.00	*1.00	*1.00

6.5 Selection of ϕ_c for Load Rating

This section is provided to simplify selection of the appropriate ϕ_c based on the information provided by the inspection. The first step is to identify the type of steel used to construct the bridge (carbon or weathering) and the environment where the bridge is located (rural, industrial, or marine conditions, consistent with NCHRP 301). This process is shown in Figure 6.13. Next, determine the type of deterioration profile (GP1 or GP2, refer to 3.2.2 Girder Deterioration Profile Models) present in the girder. If this information is unknown, GP2 can be conservatively assumed. Figure 6.14 identifies the appropriate type of approach consistent with the information available to the load rating engineer. The Special Approach is not included in Figure 6.14 because this method requires a special inspection. If the information for the Special Approach is present, Figure 6.18 can be used for the process.

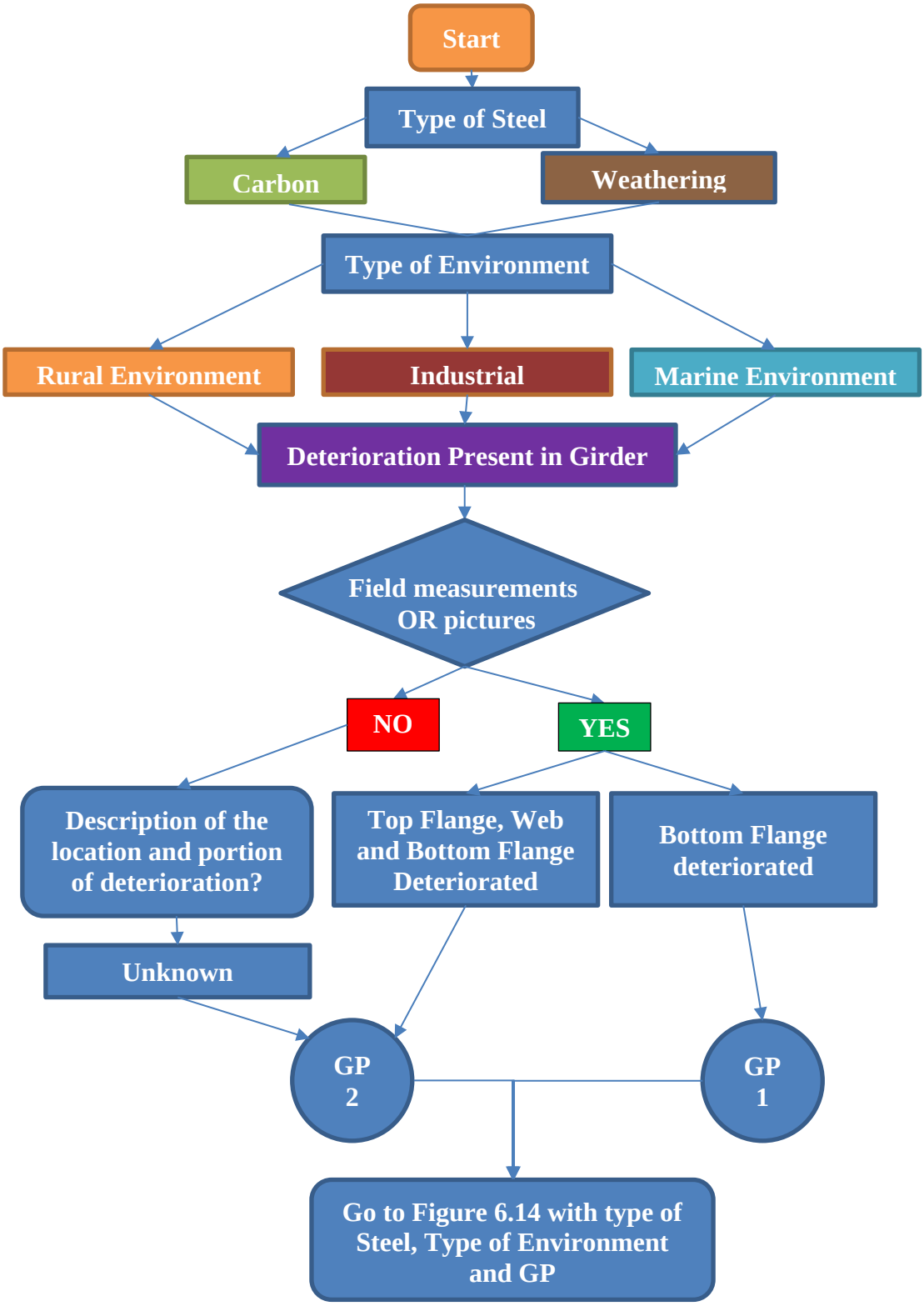

Figure 6.13 Flowchart to start the rating procedure

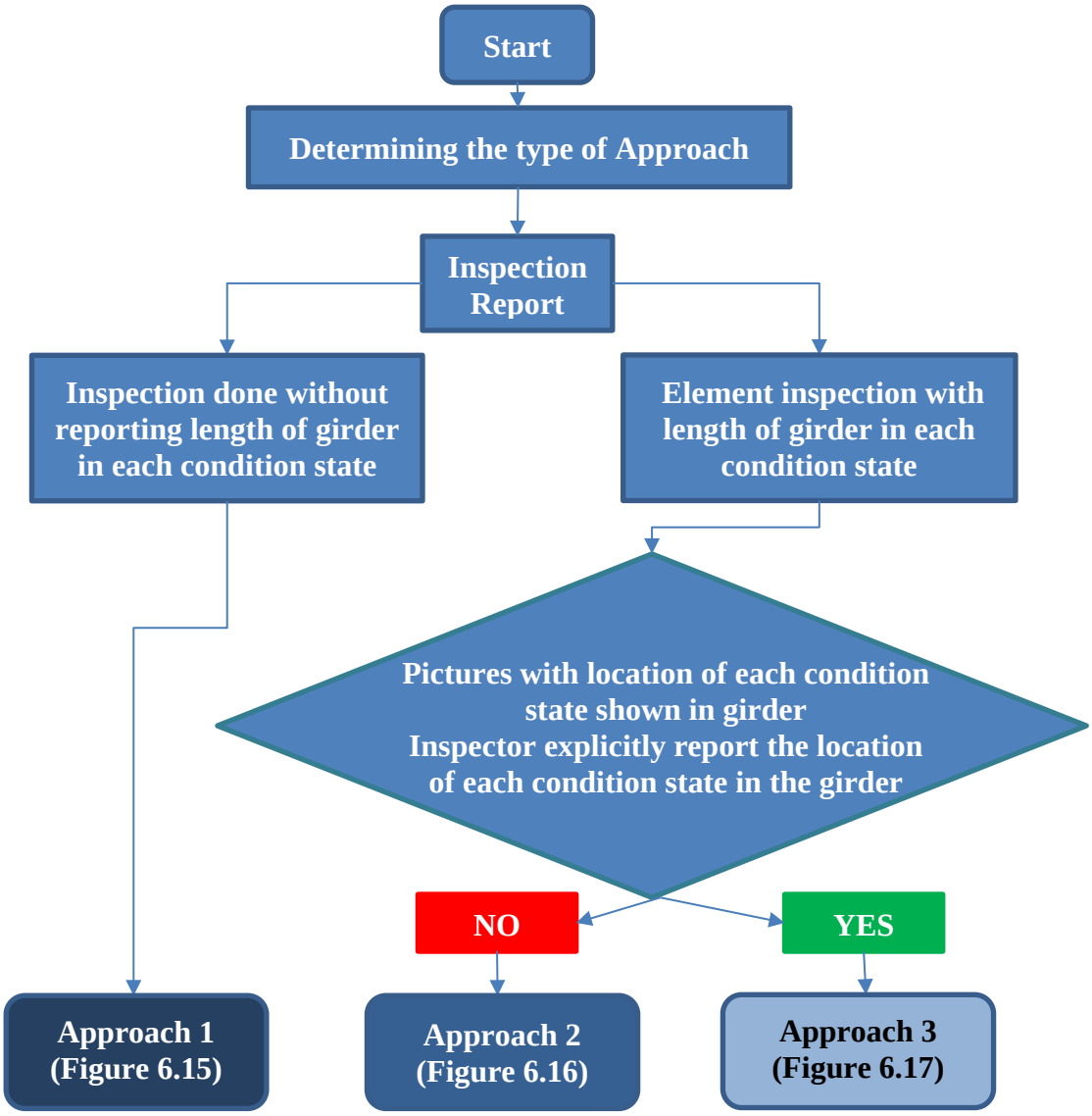

Figure 6.14 Flowchart to determine appropriate approach

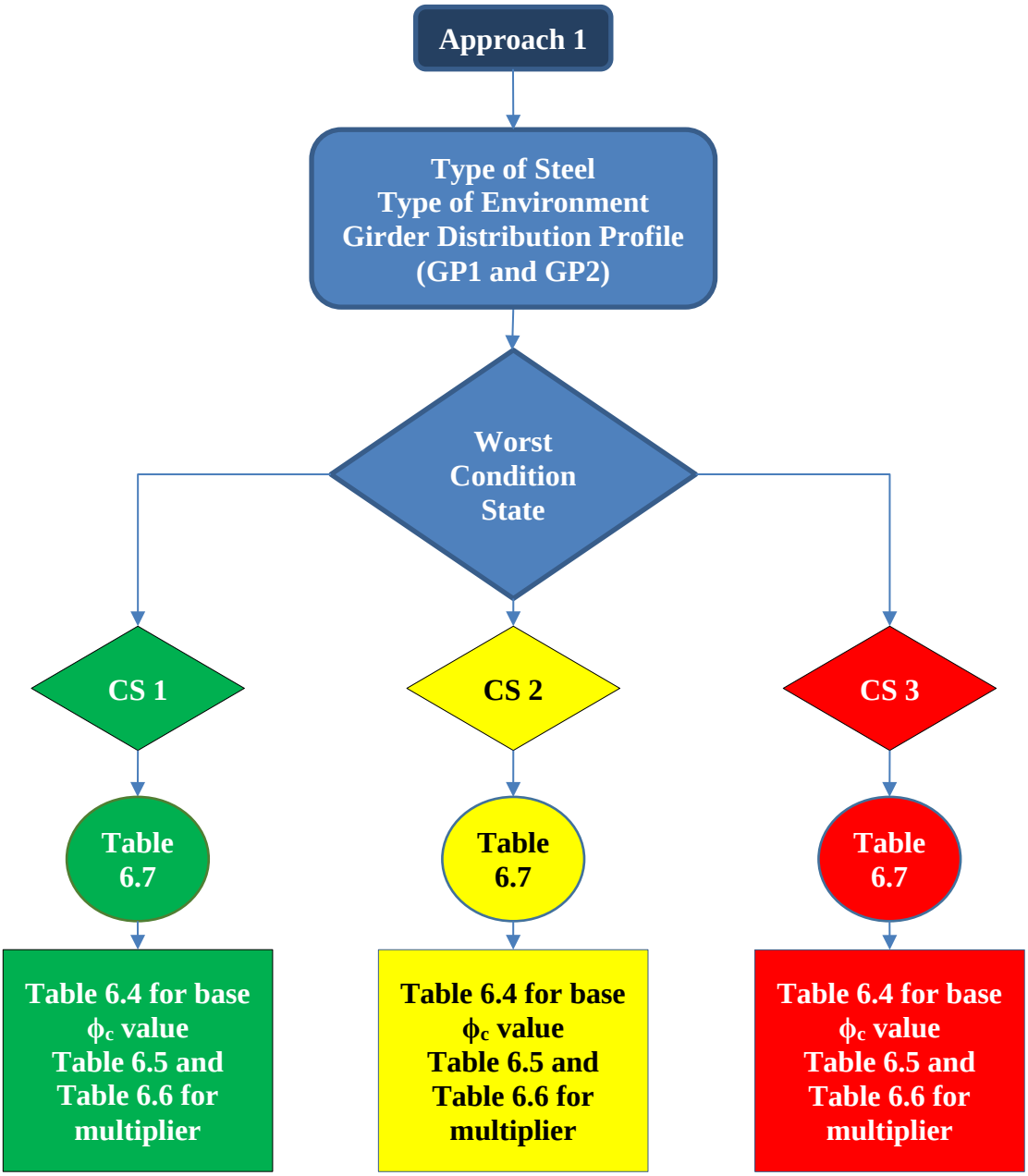

Figure 6.15 Flowchart to determine the ϕ_c for Approach 1

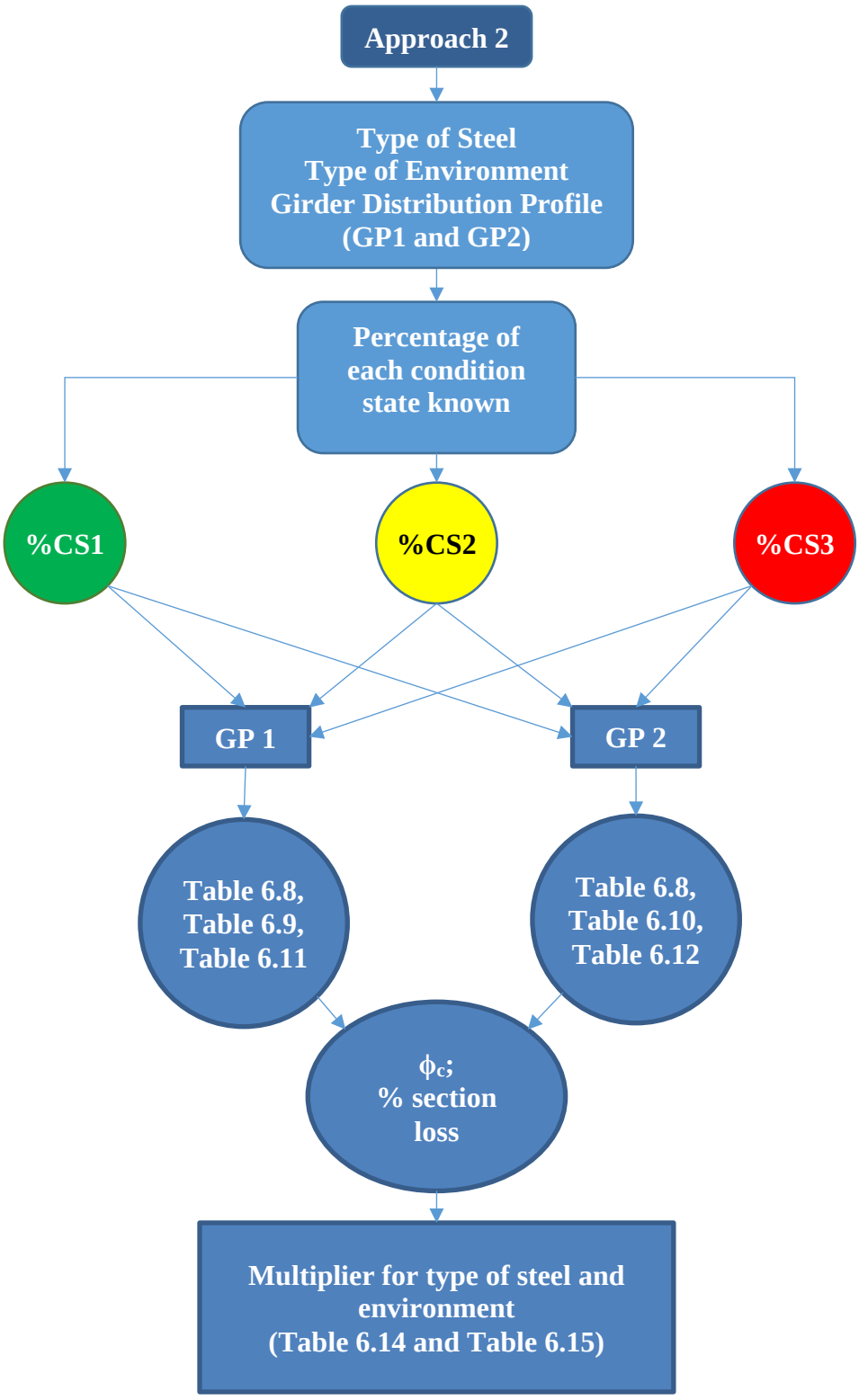

Figure 6.16 Flowchart to determine the ϕ_c for Approach 2

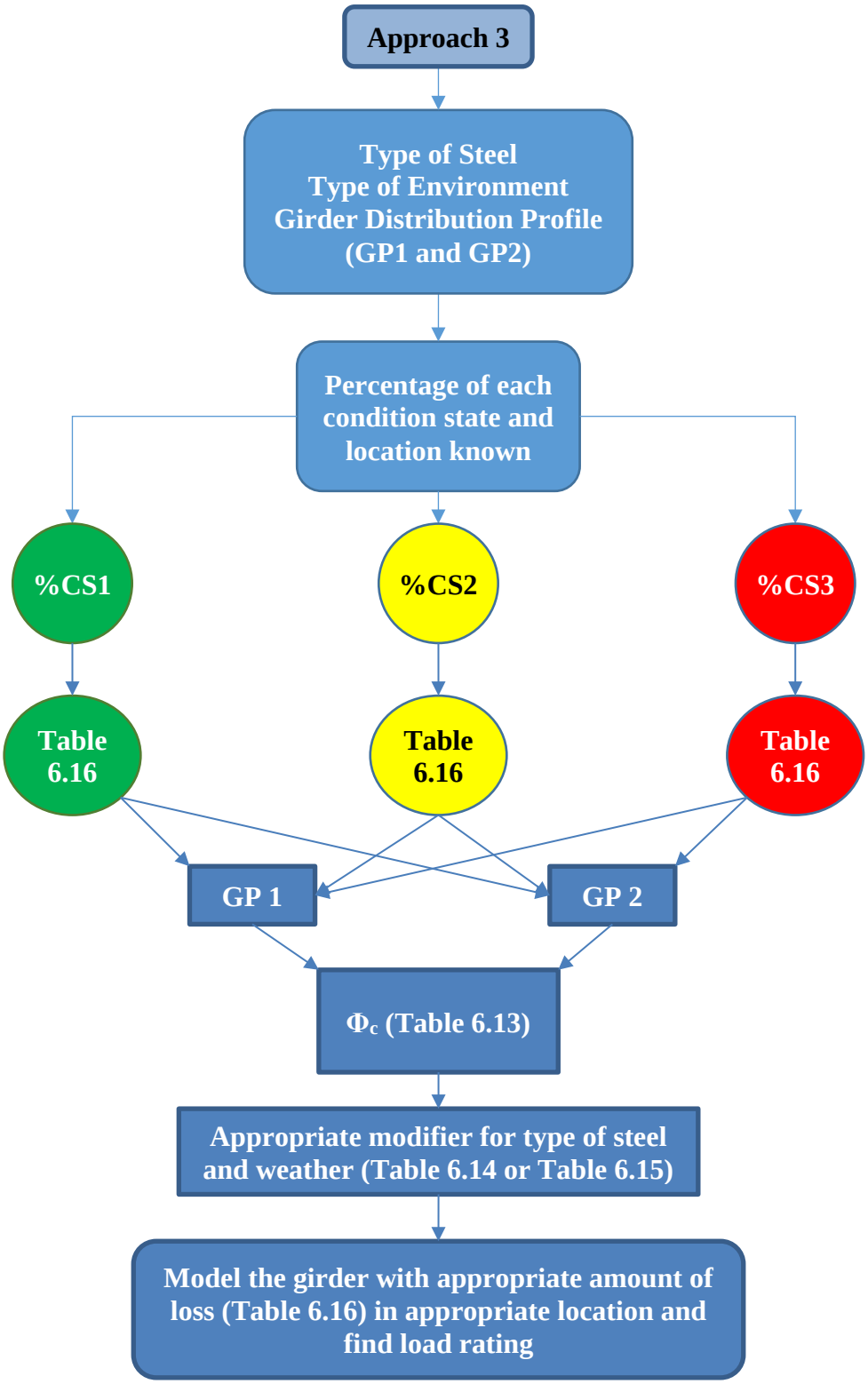

Figure 6.17 Flowchart to determine the ϕ_c for Approach 3

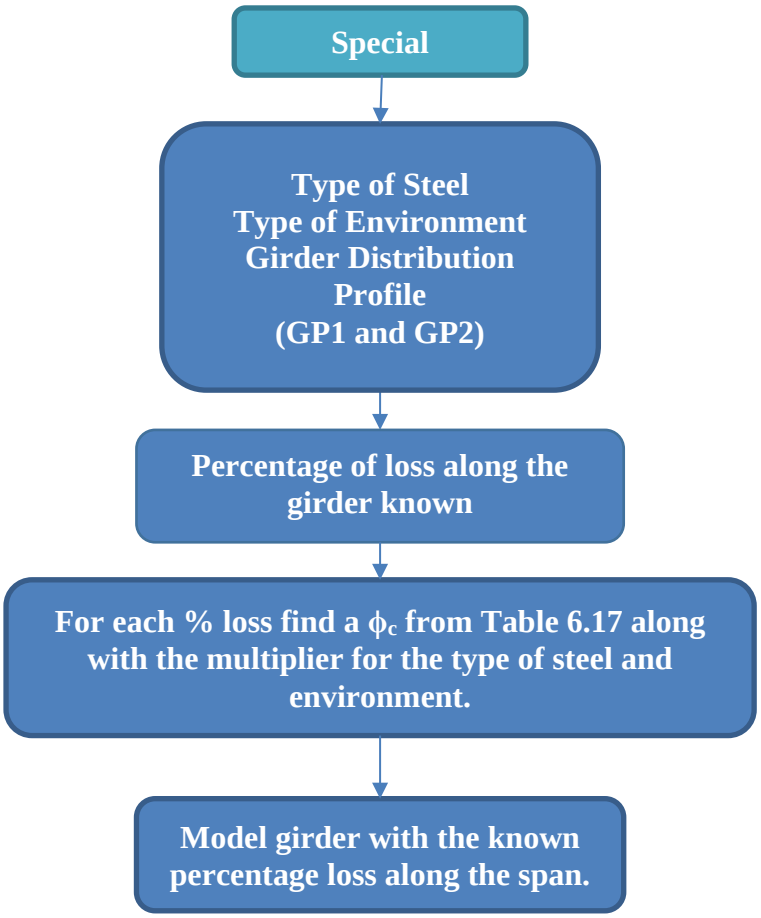

Figure 6.18 Flowchart to determine the ϕ_c for Special Approach

Chapter 7: Summary and Conclusion

Inspections provide vital information about the level of deterioration present in girders, but the information available to the load rating engineer varies throughout the inventory, resulting in unintended and unaccounted for fluctuations in rating reliability without the use of condition factors (ϕ_c). Condition factors for steel girder bridges should account for increased uncertainty in the resistance of deteriorated girders arising from non-uniform girder deterioration across a section, unknown deterioration severity (percent section loss), unknown location(s) of deterioration along the span, and potential future deterioration over the next inspection cycle. There is little objective procedural guidance at present to support reliable assignment of ϕ_c values during bridge evaluations. This research is an advancement towards an objective quantification of ϕ_c.

Bounded ranges of steel girder section loss with corresponding calibrated condition factor (ϕ_c) values have been proposed in this study for bridges containing Good, Fair, and/or Poor condition states. It is expected that a bridge assessed as Severe will receive a detailed inspection by an engineer, and the additional uncertainty associated with deteriorated conditions will be greatly diminished. The calibrated ϕ_c values account for increased uncertainty in the resistance of deteriorated steel girders and the likely future deterioration of these members between inspection cycles.

The MBEI recognizes four condition states (CS1 to CS4) corresponding approximately to Good, Fair, Poor, and Severe, respectively. Ranges of section loss were estimated based on inference from the subjective descriptions of the Good, Fair, and Poor condition states in the MBEI. These estimated ranges were referred to as NDOR's ranges, because NDOR (as well as other agencies) are currently using the subjective MBEI descriptions for inspection records. This

report presents an alternative set of ϕ_c values from those found in the MBE, in part to address the uncertainty in severity of section loss. Additionally, two alternative sets of percentage section loss ranges (for two girder deterioration profiles) are proposed, calibrated to more closely match ϕ_c values provided in the MBE.

Four approaches for varying levels of available inspection information are proposed to account for a wide range of load rating situations. Three approaches are based on the current condition state description model, which categorizes the deterioration of the girder into one of the four condition states. The fourth approach deviated from the traditional condition state model to a more detailed rating procedure based on the section loss percentage present in the girder.

The two most influential aspects of information when assigning a condition factor are: (1) location of the section loss along the spans, and (2) exact severity of section loss at a section. The unknown location of deterioration contributes substantial additional uncertainty as described in Approaches 1 and 2, lowering the ϕ_c value. The uncertainty in deterioration location can be mitigated with minimum effort during the inspection process by referring to pictures taken during inspections. Approach 3 and the Special Approach can be performed when the locations of the condition states along spans are known. In Approach 3, the description in the notes section for the portion(s) and location(s) of corrosion reduces the uncertainty in the load rating. The Special Approach requires measured values of section loss corresponding to positions along the girder lengths, resulting in the most accurate load rating.

The other primary challenge in assigning ϕ_c is the interpretation of deterioration severity by the load rating engineer, based on inspection reports. Currently, condition states are used to describe deterioration severity, but no quantitative guidance is available to inspectors or load rating engineers correlating condition states to section loss. This research suggests objective

ranges for percentage section loss due to corrosion corresponding to condition states, intended to improve uniformity in the inspection process and ensure reliable and consistent transfer of information to the load rating engineer. Approaches 1 through 3 have quantitatively and algorithmically accounted for uncertainties in a range of section loss, and therefore implicitly include this uncertainty in the proposed ϕ_c values. The Special Approach does not use traditional condition state descriptions, removing this aspect of uncertainty from the ϕ_c values with that approach.

Future research is required to address the effects of other defects present in various types of bridges. Other defects, such as cracking, have characteristic condition states that need to be objectively characterized to improve the reliability of the load rating. Condition states need to be clearly and objectively defined for all element types and associated defects in the MBEI, as has been described in this research for steel girder corrosion. Inspection records based on clear, objective definitions for condition states will facilitate consistency among ratings that provide more uniform safety throughout the inventory.

In conclusion, this research is a step towards improving the LRFR load rating procedure for structures containing appreciable deterioration. If a bridge with deterioration is carefully modeled with all its defects during load rating, the rating procedure should produce a capacity consistent with the reliability intended in LRFR. The ϕ_c in LRFR is the only factor that accounts for the increased uncertainties in the capacity of the girder due to deterioration, therefore, the use of ϕ_c is vital for consistently reliable load rating. The uncertainties associated with ϕ_c can be decreased with comprehensive inspection, which would consequently decrease the penalty by ϕ_c to achieve the target reliability in LRFR or increase the estimation of the nominal capacity. The four approaches show that penalty by ϕ_c decreases with increasing level of inspection detail.

Moving forward, inspection detail should be standardized, and additional types of defects in various elements, other than corrosion in steel girders, should be studied to extend the use of ϕ_c.

References

AASHTO. (2014). ***Manual for bridge evaluation, 2nd edition, with 2011, 2013, and 2014 Interim revisions*** (2nd edition ed.). Washington, D.C.: AASHTO.

Agatonovic-Kustrin, S., & Beresford, R. (2000). Basic concepts of artificial neural network (ANN) modeling and its application in pharmaceutical research. *Journal of Pharmaceutical and Biomedical Analysis, 22*(5), 717-727.

Albrecht, P., & Naeemi, A. H. (1984). Performance of weathering steel in bridges. *NCHRP Report,* (272)

Ambler, H., & Bain, A. (1955). Corrosion of metals in the tropics. *Journal of Applied Chemistry, 5*(9), 437-467.

ASTM International. (2011). *ASTM G103(2011) standard practice for preparing, cleaning, and evaluating corrosion test specimens*. West Conshohocken, PA: ASTM International.

ASTM International. (2015). *ASTM G5010(2015) standard practice for conducting atmospheric corrosion tests on metals*. West Conshohocken, PA: ASTM International.

Baboian, R. R. B. (2005). *Corrosion tests and standards: Application and interpretation*

Czarnecki, A. A., & Nowak, A. S. (2008). Time-variant reliability profiles for steel girder bridges. *Structural Safety, 30*(1), 49-64.

Dean, S. W. (1990). Corrosion testing of metals under natural atmospheric conditions. *Corrosion testing and evaluation: Silver anniversary volume* () ASTM International.

Federal Highway Administration. (2010). ***Federal-aid policy guide***. Washington, D.C.: U.S. Department of Transportation.

Federal Highway Administration. (2012). *Bridge inspector's reference manual*. Washington, D.C.: U.S. Department of Transportation.

Kayser, J. R., & Nowak, A. S. (1987). Evaluation of corroded steel bridges. *Bridges and Transmission Line Structures*, 35-46.

Kayser, J. R., & Nowak, A. S. (1989a). Capacity loss due to corrosion in steel-girder bridges. *Journal of Structural Engineering, 115*(6), 1525-1537.

Kayser, J. R., & Nowak, A. S. (1989b). Reliability of corroded steel girder bridges. *Structural Safety*, *6*(1), 53-63.

Komp, M. (1987). Atmospheric corrosion ratings of weethering steels—calculation and significance. *Materials Performance, 26*(7), 42-44.

Kulicki, J., Prucz, Z., Sorgenfrei, D., Mertz, D., & Young, W. (1990). *Guidelines for evaluating corrosion effects in existing steel bridges*

McCrum, R., Arnold, C. J., & Dexter, R. (1985). Current status report: Effects of corrosion on unpainted weathering steel bridges. *Current Status Report: Effects of Corrosion on Unpainted Weathering Steel Bridges,*

Moses, F., & Verma, D. (1987). In Transportation Research Board (Ed.), *NCHRP report 301: Load capacity evaluation of existing bridges*. Washington, DC:

Moses, F. (2001). *NCHRP 454: Calibration of load factors for LRFR bridge evaluation*. Washington, D.C.: Transportation Research Board.

Nebraska Department of Roads: Bridge Division. (2015). Bridge inspection program manual.

Nowak S., A., & Collins R., K. (2013). *Reliability of structures* (second ed.). Boca Raton, FL: Taylor & Francis Group.

Patras, W. (2016). *Personal communication*

Wang, N. (2010). *Reliability-Based Condition Assessment of Existing Highway Bridges,*

Weseman, W. (1995). Recording and coding guide for the structure inventory and appraisal of the nation's bridges. *United States Department of Transportation (Ed.), Federal Highway Administration, USA,*

Yunovich, M., Thompson, N., Balvanyos, T., & Lave, L. (2001). Corrosion cost and preventive strategies in the united States—Appendix d—highway bridges. *Federal Highway Administration, FHWA-RD-01-157,*

Zmetra, K., Zaghi, A. E., & Wille, K. (2015). Rehabilitation of steel bridge girders with corroded ends using ultra-high performance concrete. *Structures Congress 2015*